

# The *Drosophila* NCAM homolog Fas2 signals independent of adhesion

Helen Neuert<sup>1,2</sup>, Petra Deing<sup>1</sup>, Karin Krukkert<sup>1</sup>, Elke Naffin<sup>1</sup>, Georg Steffes<sup>1</sup>,  
Benjamin Risse<sup>1,3</sup>, Marion Silies<sup>1,4</sup>, and Christian Klämbt<sup>1,5,6</sup>

1) University of Münster, Institute for Neuro- and Behavioral Biology, Badestr. 9,  
48149 Münster, Germany

2) present address: University of British Columbia, Department of Cellular and  
Physiological Sciences, 2350 Health Sciences Mall, Vancouver BC V6T 1Z3, Canada

3) present address: University of Münster, Institute for Informatics, Einsteinstraße 62,  
48149 Münster, Germany

4) present address: Johannes-Gutenberg-University of Mainz, Institute of  
Development Biology and Neurobiology, Hanns-Dieter-Hüsck Weg 15, 55099 Mainz,  
Germany

5) Corresponding Author: [klaembt@uni-muenster.de](mailto:klaembt@uni-muenster.de)

6) Lead Contact: [klaembt@uni-muenster.de](mailto:klaembt@uni-muenster.de)

Keywords: NCAM, Fasciclin 2, *Drosophila*, GPI-anchor, adhesion, isoform specific  
mutants, glial migration

## Abstract

The development of tissues and organs requires close interaction of cells. To do so, cells express adhesion proteins such as the neural cell adhesion molecule (NCAM) or its *Drosophila* orthologue Fasciclin 2 (Fas2). Both are members of the Ig-domain superfamily of proteins that mediate homophilic adhesion. These proteins are expressed as different isoforms differing in their membrane anchorage and their cytoplasmic domains. To study the function of single isoforms we have conducted a comprehensive genetic analysis of *fas2*. We reveal the expression pattern of all major Fas2 isoforms, two of which are GPI-anchored. The remaining five isoforms carry transmembrane domains with variable cytoplasmic tails. We generated *fas2* mutants expressing only single isoforms. In contrast to the null mutation which causes embryonic lethality, these mutants are viable, indicating redundancy among the different isoforms. Cell type specific rescue experiments showed that glial secreted Fas2 can rescue the *fas2* mutant phenotype to viability. This demonstrates cytoplasmic Fas2 domains have no apparent essential functions and indicate that Fas2 has function(s) other than homophilic adhesion. In conclusion, our data propose novel mechanistic aspects of a long studied adhesion protein.

## Introduction

The development of complex organism requires manifold concerted interactions of the cellular building blocks. These interactions in part depend on regulated adhesion which is in particular necessary in the nervous system (Silies and Klämbt, 2011).

Here neurons form intricate networks where uncountable specific cellular connections provide the hardware of neuronal computation (Eichler et al., 2017; Larderet et al., 2017; Schneider-Mizell et al., 2016). Full functional complexity of the brain, however, then requires glial cells which interact among each other and with neurons to perform a multitude of different tasks required for neuronal function (Yildirim et al., 2018). The close cell-cell interactions observed in the nervous system are based on two properties. Cell-cell contacts and adhesion need to be specified to ensure the formation of stable connections and subsequently allow cell-cell signaling and communication. Cell communication is exemplified by chemical synapses, where neurons exchange information by secreting and receiving transmitter molecules. In addition, neurons can communicate in manifold ways with glial cells (Gundersen et al., 2015). In most cases neuron-glia interaction depends on a close contact of the respective cells. Therefore, adhesion proteins are of particular relevance to allow the interaction between different cell types.

Both homophilic or heterophilic adhesions can mediate cellular interactions. An example of the latter type is Amalgam, a secreted adhesion protein with three tandem immunoglobulin (Ig)-domains. In solution, Amalgam forms dimers that cross-link Neurotactin proteins expressed on the surfaces of opposing cells (Fremion et al., 2000; Liebl et al., 2003; Zeev-Ben-Mordehai et al., 2009). Similarly, heterophilic interaction is reported for NeurexinIV / Caspr which - depending on an alternatively spliced exon - can either bind the Ig-domain protein Wrapper or Contactin, another

Ig-domain protein (Noordermeer et al., 1998; Stork et al., 2009; Wheeler et al., 2009). Homophilic interactions are for example mediated by the *Drosophila* Ig domain protein Neuroglian (Nrg), which constitutes the *Drosophila* homolog of the vertebrate L1 Ig-domain adhesion protein. Interestingly, different Nrg / L1 isoforms are characterized by distinct cytoplasmic domains and have been evolutionary conserved. These two adhesion proteins (Nrg167 and Nrg180 in the fly) are expressed by either glial or neuronal cells and in both cell types provide the link to the actin cytoskeleton via common adaptor proteins (Bieber et al., 1989; Chen and Hing, 2008; Hortsch et al., 1990; Yamamoto et al., 2006). Another well studied homophilic adhesion protein known in vertebrates and invertebrates is NCAM or Fasciclin2 (Fas2). Fas2 was originally discovered as a motor axon marker that was subsequently shown to mediate activity dependent expansion of the neuromuscular junction (Davis et al., 1997; Schuster et al., 1996a; Schuster et al., 1996b; Thomas et al., 1997).

Fas2 / NCAM are evolutionary very well conserved. Interestingly, *NCAM* mouse mutants are viable and fertile with only minor nervous system phenotypes (Cremer et al., 1994b). In contrast, *Drosophila fas2* mutants are early larval lethal and display some morphological phenotypes at the developing neuromuscular junction (Kohsaka et al., 2007; Kristiansen and Hortsch, 2008; Schuster et al., 1996a; Schuster et al., 1996b). A dynamic role of Fas2 has been suggested to allow neuronal plasticity influencing circadian behavior (Sivachenko et al., 2013). Importantly, both, Fas2 and its vertebrate homolog NCAM, are involved in neuron-glia signaling (Higgins et al., 2002; Paratcha et al., 2003; Wright and Copenhaver, 2001). In *Drosophila*, a graded expression of Fas2 on motor axons is needed for peripheral glial migration (Silies and Klämbt, 2010). Although gain of Fas2 expression clearly halts glial cell migration, glial migration appears normal in *fas2* null mutants. Outside of the nervous system

Fas2 is needed for microvilli length and organization in the Malpighian tubules stabilizing the brush border possibly requiring homophilic adhesion (Halberg et al., 2016). The *fas2* gene is predicted to encode at least seven differentially expressed isoforms. As known for NCAM, the different Fas2 isoforms differ mostly in their membrane attachment and the cytoplasmic domain. However, despite the wealth in genomic information on the different Fas2 isoforms, their possible individual contribution is not known in any context.

Here we have conducted a comprehensive genetic analysis of the different *fas2* isoforms to decipher their relative contributions during development. Our data reveals that only the GPI-anchored Fas2<sup>PB</sup> affects glial migration but otherwise highly redundant functions of all isoforms were identified. Interestingly, both neuronal expression of transmembrane anchored Fas2<sup>PD</sup> as well as glial expression of secreted Fas2 rescues the lethal *fas2* phenotype, suggesting that Fas2 can act independent of its homophilic adhesion functions.

## Results

### Distinct *fasciclin 2* isoforms are GPI anchored

The *fasciclin 2* (*fas2*) gene spreads over 75 kbp and encodes a series of evolutionary conserved immunoglobulin (Ig)-domain proteins (Figure 1A-C). Currently seven mRNA splice variants encoding 7 distinct proteins are described (Fas2<sup>PA</sup>, Fas2<sup>PB</sup>, Fas2<sup>PC</sup>, Fas2<sup>PD</sup>, Fas2<sup>PF</sup>, Fas2<sup>PG</sup>, and Fas2<sup>PH</sup>, Figure 1A,B; FlyBase). To verify the presence of the predicted splice variants we extracted total mRNA from wild type embryos and performed RT-PCR reactions with isoform specific primer pairs (Figure 1D). cDNA corresponding to all seven isoforms could be amplified with isoforms RB, RC and RF being predominant (Figure 1D).

The different Fas2 isoforms are predicted to be either transmembrane proteins or tethered to the membrane via GPI anchors but real experimental evidence for the latter is missing. Isoforms PA, PD, PG, PH and PF all share one common exon that is absent from PB and PC (Figure 1A,B). Of the former isoforms PA is as the PD isoform but in addition carries a cytoplasmic PEST domain. This PEST domain is also present in isoform PG, which contains additional 12 amino acids in the cytoplasmic domain. The PH isoform carries a unique cytoplasmic domain of 27 amino acids, and the isoform PF is generated by adding 15 amino acids to the first Ig-domain of the PD isoform (Figure 1A,B).

The isoform PC is predicted to have a transmembrane anchor (SMART, smart.embl-heidelberg.de), however, it had been suggested that Fas2<sup>PC</sup> is linked to the plasma membrane by a GPI anchor (Grenningloh et al., 1991). The isoform PB lacks a clear transmembrane domain and a GPI anchor is predicted by a Kohonen self-organizing map, GPI-SOM, (Fankhauser and Mäser, 2005).

To experimentally determine the membrane anchorage of Fas2<sup>PB</sup> and Fas2<sup>PC</sup> we generated HA-tagged cDNA clones and expressed the proteins in S2 cells. HA-Fas2<sup>PB</sup> and HA-Fas2<sup>PC</sup> were found in cell lysates at the expected size of 90 kDa in western blots (Supplementary Figure 1). Minor amounts of both Fas2 protein isoforms are released from the cell membrane and can be detected in the supernatant. To test whether the proteins are linked to the plasma membrane via a GPI-anchor, we added PiPLC to the cell culture medium. This enzyme, which specifically cleaves GPI-anchors (Heinz et al., 1998), was able to efficiently solubilize HA-Fas2<sup>PB</sup> as well as HA-Fas2<sup>PC</sup> protein which was then found in the supernatant (Supplementary Figure 1). This demonstrates that the Fas2 isoforms, PB and PC, are attached to the plasma membrane by a GPI-anchor. The exon common to all

other isoforms (PA, PD, PF, PG, and PH) contains a transmembrane domain and therefore, we will refer to these isoforms together as Fas2<sup>TM</sup> (Figure 1C).

### **Fas2 isoforms are differentially expressed**

In order to detect Fas2 protein expression within the developing nervous system, we utilized a number of protein trap insertion lines and one MiMIC strain which we used to insert a monomeric Cherry (*mCherry*) encoding exon (*MiMIC12989* (Nagarkar-Jaiswal et al., 2015); Figure 1A, Figure 2). The insertion of a *mCherry* encoding exon in *MiMIC12989* (*fas2<sup>MiMIC12989::mCherry</sup>*) reduced fitness but a homozygous stock could be established.

Three *fas2* insertion lines are available that in principle should detect the expression of all isoforms (*fas2<sup>GFP778</sup>*, *fas2<sup>CPTI000483</sup>* (Lowe et al., 2014) and *fas2<sup>MiMIC12989::mCherry</sup>*).

During embryogenesis, the protein trap insertion *CPTI000483* directs robust expression in a subset of neurons. In addition, weak expression is detected in ectodermal cells (Figure 1E,F). A similarly broad GFP expression pattern is associated with the protein trap insertion *fas2<sup>GFP778</sup>*, in the embryo as well as in the larval nervous system (Supplementary Figure 2). In *fas2<sup>MiMIC12989::mCherry</sup>* animals, broader Cherry expression could be detected, suggesting that the position of the additional GFP exon present in *CPTI000483* and *fas2<sup>GFP778</sup>* affects splicing probability in the different cell types, and *fas2<sup>MiMIC12989::mCherry</sup>* is providing a better read-out of Fas2 expression (Figure 2). In *fas2<sup>MiMIC12989::mCherry</sup>* embryos, expression could be noted in a subset of neurons but is also seen in the epidermis, the Malpighian tubules, the midgut, and in glial cells (Figure 2A-H). This exon trap thus reveals that Fas2 is more broadly expressed than previously known.

The exon trap insertion line *fas2<sup>GFP397</sup>* labels all expression domains except the one of *fas2<sup>RC</sup>*. It revealed strong GFP expression in the nervous system, including

expression in glial and epidermal cells (Figure 1G,H; (Silies and Klämbt, 2010)). The insertion *CPT1001279* (Lowe et al., 2014) results in GFP labeling of isoforms PA, PD, PG, and PH, and shows an exclusive neuronal expression pattern which also corresponds to the expression pattern detected by the monoclonal antibody mAb 1D4 (Grenningloh et al., 1991) (Figure 1I,J). The difference between these two expression patterns can therefore be allocated to isoform PB, arguing that PB is expressed in glial cells, and other tissues.

A similar expression as observed in *CPT1001279* is detected by the insertion *CB03613* which labels some but not all transmembrane isoforms. This insertion disrupts the PEST domain encoding exon and shows an only neuronal expression (Figure 1K,L). Very similar expression profiles were detected during larval stages (Figure 2, Supplementary Figure 2). The two insertion lines *fas2<sup>GFP778</sup>* and *fas2<sup>CPT1000483</sup>* that in principle should detect expression of all isoforms are mostly expressed in neurons with some epidermal expression. No clear glial expression was seen (Supplementary Figure 2A-D,E-H). In contrast, *fas2<sup>MiMIC12989::mCherry</sup>* also showed clear neuronal and glial Fas2 expression. In the third instar brain, surface glial cells expressed *Fas2<sup>MiMIC12898::mCherry</sup>*, but the broad expression pattern did not allow to discriminate between perineurial and subperineurial glial cells. In addition, the ensheathing glia that surround the neuropil expressed *Fas2<sup>MiMIC12898::mCherry</sup>* (Figure 2I-L). In the eye-imaginal disc, strongest *Fas2<sup>MiMIC12898::mCherry</sup>* expression was noted in photoreceptor cells. Expression could also be detected in glial cells, which could be identified as perineurial glial cells based on their position at the base of the eye disc (Figure 2M,N). The insertion *fas2<sup>GFP397</sup>* showed clear ectodermal expression in leg and eye-antennal imaginal discs and also revealed glial expression (Supplementary Figure 2I-L). As noted in the embryo, *CPT1001279* and *CB03613* directed expression exclusively in neuronal cells (Supplementary Figure 2M-P,Q-T).



In summary, Fas2 is more broadly expressed than previously thought, and Fas2<sup>MiMIC12898::mCherry</sup> presents a useful tool to study the full Fas2 expression pattern. Whereas the transmembrane anchored Fas2 proteins PA, and PD-PH appear to have a purely neuronal expression profile, the GPI-anchored isoform PB also shows additional glial and epidermal expression. In addition, isoform PC is also found in the tracheal system (see below). Importantly, all differences in Fas2 isoform expression are due to differential splicing in the different cell types.

### **Generation of a molecularly and genetically defined *fas2* null mutant**

A previously generated, transposon excision-induced *fas2* allele, *fas2*<sup>EB112</sup>, carries a 1.7 kbp deletion in the presumed *fas2* promoter region. *fas2*<sup>EB112</sup> homozygous mutant animals die as early first instar larvae and expression of Fas2<sup>TM</sup>, which can be detected by the monoclonal antibody 1D4, is absent (Grenningloh et al., 1991). Given that this antibody misses the expression of other isoforms, and it was unclear whether the promoter deletion would also affect the expression of all other isoforms, we generate a molecularly clearly defined *fas2* null allele. We performed a recombination based approach (Parks et al., 2004) employing FRT elements residing in *P{XP}d07035*, inserted 300 bp upstream of the presumed transcriptional start site, and *PBac{WH}f06654*, inserted downstream of the *fas2* locus (Figure 2A). Thereby a small deletion covering the entire *fas2* gene locus plus one additional gene, *GlcAT-I*, was generated (Figure 3A). *GlcAT-I* encodes a glycosyltransferase which is ubiquitously expressed throughout development (Kim et al., 2003). A PBac insertion in the 5' UTR of *GlcAT-I* is viable and fertile in homozygosis (FlyBase). In contrast, hemizygous *Df(1)fas2* animals are early first instar larval lethal with no detectable Fas2 protein expression. The identical lethal phases and the same glial migration phenotype (see below) noted for both *fas2* alleles indicates that the classic *fas2*<sup>EB112</sup>

is indeed a *fas2* null allele, and the observed phenotypes are due to loss of *fas2* function.

### **Fas2 can act without its cytoplasmic domain**

We next asked if all or if specific *fas2* isoforms were required for the lethality caused by loss of *fas2*. We used molecularly defined chromosomal duplications to test the genetic requirements of *fas2*. BAC based duplications are stretches of genomic DNA with an average length of 88 kb. Many of these constructs are inserted in the same landing site on chromosome 3L, allowing their direct comparison (Venken et al., 2010). Four duplications were tested *Dp(1;3)DC115*; *Dp(1;3)DC465*; *Dp(1;3)DC075*, and *Dp(1,3)Fas2* which we generated by integrating the BAC clone *CH321-75A18* into the landing site *VK33* (Figure 3A). Except *Dp(1;3)DC075*, all duplications cover the entire *fas2* gene with all exons but differ in the length of 5' sequences.

*Dp(1;3)DC075* lacks the exons located on the 3' end of the *fas2* gene resulting in a construct that only expresses the Fas2<sup>PC</sup> isoform (Figure 3A).

Except *Dp(1;3)DC075*, all duplications fully rescue the lethality associated with *fas2*<sup>EB112</sup>. Interestingly, *Dp(1;3)DC115* harbors only little 5' sequences upstream of the predicted promoter suggesting that most regulatory sequences reside in intronic regions. The presence of *Dp(1;3)DC075* alone still provided a partial rescue with 10% of the expected number of hemizygous flies appearing (17 *fas2*<sup>EB112</sup> / Y; *Dp(1;3)DC075* males and 164 FM7 / Y: *Dp(1;3)DC075* males). This argues that a GPI-anchored isoform alone can fulfill important Fas2 functions. To test this more explicitly, we used genome editing to generate a CRISPR induced mutation leaving only isoform Fas2<sup>PC</sup> intact (*fas2*<sup>ΔPB, ΔTM</sup>) (see Materials and Methods). This mutant is fully viable with no obvious discernible phenotypes at this level of resolution (Figure 4). The rescue ability of the *Dp(1;3)DC075* duplication might be not as effective since

the mRNA may be truncated due to the nature of the construct and is possibly not as stable as the mRNA generated from the CRISPR induced allele. In conclusion, however, both experiments suggest that expression of only the GPI-anchored isoform Fas2<sup>PC</sup> is sufficient to restore viability.

### **Fas2 can act independent of its homophilic adhesion properties**

In addition, we performed an isoform specific overexpression approach for rescue experiments (see Materials and Methods for details). Several transgenes encoding different Fas2-YFP proteins have been published (Kohsaka et al., 2007). Expression of wild type, YFP-tagged transmembrane Fas2<sup>PD</sup> protein in neurons and muscle cells rescued the lethality associated with the *fas2*<sup>EB112</sup> mutant (Kohsaka et al., 2007).

In a next step, we expressed YFP-tagged Fas2<sup>PD</sup> specifically in glial cells using the *repo-Gal4* driver. Glial expression of the transmembrane *fas2* transgene did not rescue the lethality of *fas2* mutants. In a cross of [*fas2*<sup>EB112</sup>/FM7; *UAS-fas2*<sup>PD-YFP</sup> X *repo-Gal4*] we found 63 FM7 males and no *fas2*<sup>EB112</sup> male. However, quite surprisingly, expression of a secreted Fas2 protein lacking all membrane anchorage sequences (Kohsaka et al., 2007) only in glial cells was able to rescue some animals to fully viable and fertile males. From the cross [*fas2*<sup>EB112</sup>/FM7; *UAS-fas2*<sup>extra-YFP</sup> X *repo-Gal4*] we found 167 FM7 males and 10 fertile males [genotype: *fas2*<sup>EB112</sup>/Y, *UAS-fas2*<sup>extra-YFP</sup>; *repo-Gal4*]. Likewise, neuronal expression of *Fas2*<sup>extra-YFP</sup> alone is able to only weakly rescue the lethal *fas2* phenotype. From the cross [*fas2*<sup>EB112</sup>/FM7; *UAS-fas2*<sup>extra-YFP</sup> X *nsyb-Gal4*] we found 143 FM7 males and 5 fertile males of the genotype: [*fas2*<sup>EB112</sup>; *UAS-fas2*<sup>extra-YFP</sup>; *nsyb-Gal4*]. Since expression of a secreted Fas2 protein only in glial cells can also rescue lethality, we conclude that Fas2 does not strictly require a homophilic adhesive interaction to perform its essential role during development.

## Genome editing generates isoform specific *fas2* mutants

The P-element *fas2*<sup>CB03613</sup> (Buszczak et al., 2007) is inserted within an exon incorporated in Fas2<sup>PA</sup> and Fas2<sup>PG</sup>. Thus, the insertion disrupts at least the function of Fas2<sup>PA</sup> and Fas2<sup>PG</sup>. Hemizygous as well as homozygous flies are viable. To further delineate the requirement of the different Fas2 isoforms we first generated a deficiency chromosome where only the GPI anchored Fas2<sup>PB</sup> and Fas2<sup>PC</sup> proteins are present (*Df(1)fas2*<sup>Δ<sup>TM</sup></sup>, Figure 3A), again using FRT-mediated recombination (Parks et al., 2004). Whereas expression of the isoform Fas2<sup>TM</sup> specific mAb 1D4 epitope is visible in heterozygous *Df(1)fas2*<sup>Δ<sup>TM</sup></sup> embryos (Figure 3B,C), it is absent from all homozygous tissues tested (Figure 3D-K), confirming the loss of all isoforms carrying the large cytoplasmic domain. *Df(1)fas2*<sup>Δ<sup>TM</sup></sup> flies producing only GPI-anchored Fas2 proteins are viable and fertile in homozygosis with a reduced fitness compared to the balancer carrying heterozygous animals. This argues that the transmembrane tethered Fas2 isoforms and their cytoplasmic domains are not strictly required. Together, these data suggest that no signaling function originates from the cytoplasmic Fas2 domain to ensure viability.

In a next step, we utilized CRISPR/Cas9 based genome editing to induce further isoform specific mutants by generating small deletions in the respective exons (see Materials and Methods). In all cases the design of the sgRNA was aimed to disrupt the membrane anchorage sequences of the different Fas2 isoforms: either the predicted GPI anchor site of PB or PC, or the transmembrane domain common to all other isoforms (Figure 4A). A mutation in the exon that is specific for the isoform Fas2<sup>PC</sup> caused a frameshift with a stop codon at amino acid position 742. Since this mutation removes the predicted hydrophobic domain needed for GPI-anchorage it is expected to result in a secreted Fas2<sup>PC</sup> protein (*fas2*<sup>Δ<sup>PC</sup></sup>, see materials and methods

for details for all mutants generated). These mutants were homozygous viable and fertile and expression of Fas2<sup>TM</sup> as recognized by the 1D4 mAb was normal at this level of resolution (Figure 4A-D). A mutation of the exon encoding a Fas2<sup>PB</sup> specific GPI-anchor attachment site is also predicted to result in a secreted Fas2<sup>PB</sup> isoform. Hemizygous or homozygous flies lacking GPI-anchored Fas2<sup>PB</sup> were fully viable (*fas2<sup>ΔPB</sup>*, Figure 4A,B,E,F). However, we noted a change in the expression of the 1D4 antigen (which is only present in Fas2<sup>TM</sup>) and mutant embryos display a glial migration phenotype during embryonic development (see below).

### **Fasciclin 2 expression in isoform specific *fas2* mutants**

We next sought to test how the loss of specific isoforms affects the expression of other isoforms. To visualize the expression of the Fas2 isoforms PB, PA, PD-PH in the mutant backgrounds that we generated, we utilized the *fas2<sup>GFP397</sup>* exon trap strain which confers broad expression in glial and neuronal cells as can be seen best on the segmental nerves in the embryo (Figure 5A-C). We then generated a CRISPR/Cas9 mediated small deletion in the exon encoding the transmembrane domain in the *fas2<sup>GFP397</sup>* background ( $\Delta$ TM, see Figures 1,4A), blocking the membrane anchorage of PA, PD-PH and thereby generating a predicted secreted Fas2 protein. In the absence of the transmembrane anchored proteins Fas2<sup>TM</sup>, we noted robust expression of Fas2<sup>GFP</sup> along glial cells accompanying the peripheral nerves (Figure 5D-F). To test how glial Fas2 expression interacts with axonal Fas2 expression, we next generated a CRISPR/Cas9 mutant specifically affecting the GPI-anchorage of Fas2 in the *fas2<sup>397</sup>* background. In the absence of the GPI-anchorage of the Fas2<sup>PB</sup> protein, glial expression was gone, but neuronal expression of the Fas2<sup>GFP</sup> protein was still present (Figure 5G-I). Similar *fas2<sup>GFP397</sup>* expression patterns could be detected during larval stages (Supplementary Figure 3A-E). Control

*fas2<sup>GFP397</sup>* eye-imaginal discs show a glial and a neuronal expression domain (Figure 5J,K). Upon genetic ablation of the GPI-anchored *Fas2<sup>PB</sup>* form, the neuronal expression of *Fas2* remained (Figure 5L-O), whereas ablation of the neuronally expressed *Fas2* proteins revealed the glial expression domain (Figure 5P,Q). In the third instar larval nervous system, expression was more diffuse and could not be easily assigned to glial or neuronal cell types (Supplementary Figure 3F-J). The GFP signal may also originate from the *Fas2<sup>TM::GFP</sup>* isoforms that are now being secreted into the extracellular space. Consistent with this, in the eye-imaginal disc, strong expression of secreted *Fas2*, trapped between peripodial membrane and disc epithelium, could be detected (Supplementary Figure 3H,K-M). Together, these data further support neuronal expression of transmembrane *Fas2* and glial expression of GPI-anchored *Fas2<sup>PB</sup>*. Moreover, expression in one cell type can be maintained without *Fas2* expression in the other cell type.

### ***Fas2<sup>PC</sup>* is expressed in trachea which are defective in *fas2* mutant embryos**

To determine the expression pattern of *Fas2<sup>PC</sup>* we inserted a short stretch of genomic DNA harboring a *fas2<sup>PC</sup>* exon tagged with V5 and a *fas2<sup>PB</sup>* exon tagged with HA into the *fas2<sup>MiMIC12989</sup>* insertion (see Figure 6A). Using these transgenic reporter lines, we noted *Fas2<sup>PC</sup>* expression in tracheal cells (Figure 6B-E) and a small subset of neuronal cells (Figure 6F-I). During larval stages, weak expression in glial cells could be detected in the eye-imaginal discs. In addition, expression was noted in the morphogenetic furrow of the eye-imaginal disc, in young photoreceptor neurons and in a crescent of larval brain cells that might correspond to the forming lamina (Figure 6J-L). The embryonic expression pattern of *Fas2<sup>PC</sup>* prompted us to reanalyze the lethal phase of *fas2* null mutants. *fas2<sup>EB112</sup>* hemizygous embryos develop normally to stage 16 and move extensively in the egg shell suggesting that neuromuscular

junctions are established and functional. Whereas control animals hatch after 24 h development, mutant *fas2* larvae move in the egg shells but never manage to hatch. Even after 48 h the mutant animals are still moving but cannot hatch. We found that the trachea is not inflated with air in *fas2<sup>EB112</sup>* mutants which likely causes hypoxia (Figure 7).

### **GPI-anchored Fas2 isoforms are needed for glial migration**

While neuronal expression is broadly intact when glial expression is lost, interaction between neuronal and glial Fas2 might still be needed for coordinated interaction between the two cell types. A hallmark of Fas2 expression is the graded expression of Fas2<sup>TM</sup> along motor axons (Figure 8A-C,M). This gradient of neuronal Fas2 expression was previously shown to be required for the migration of peripheral glial cells during embryogenesis (Silies and Klämbt, 2010). To quantify the graded axonal distribution of Fas2 we determined the Fas2 expression in 2-6 hemisegment and then calculated the mean of Fas2 intensity ratio per embryo which was used for subsequent statistical analysis. In brief, at the onset of glial migration during stage 14, 1.79 times more Fas2 is incorporated at the growing tip of the axon compared to the axonal membrane at the CNS/PNS transition zone (Figure 8M). Interestingly, deletion of the Fas2<sup>PB</sup> isoform was sufficient to level the graded distribution of Fas2<sup>TM</sup> along motor axons (*fas2<sup>ΔPB</sup>*, Fas2 expression intensity ratio of 1.26 along the axon; Figure 8D-F,M). Given the above finding that Fas2<sup>PB</sup> is a glial expressed protein, this implies that glial cells are able to affect the graded expression of a cell adhesion protein along motor axons. To further test this hypothesis we followed the expression of Fas2<sup>TM</sup> in *Df(2L)200* mutants which removes both *glial cells missing 1* and *glial cells missing 2* and thus lack all glial cells (Hosoya et al., 1995; Jones et al., 1995; Kammerer and Giangrande, 2001; Vincent et al., 1996). In these embryos, the

gradient of neuronal Fas2<sup>TM</sup> expression was also strongly affected (Fas2 expression intensity ratio of 1.03 along the axon; Figure 8G-I,M), suggesting that a trans-interaction between glial cells and neurons is needed to set up the graded distribution of Fas2<sup>TM</sup> along the axons.

We then tested whether loss of any of the two GPI-anchored isoforms is required for a proper distribution of axonal Fas2 and tested if the isoform Fas2<sup>PC</sup> also affects the distribution of the Fas2<sup>TM</sup> isoform. In *fas2<sup>APC</sup>* mutants only a slight change in the establishment of the Fas2<sup>TM</sup> gradient along motor axons can be detected (Fas2 intensity ratio 1.49; Figure 8J-L,M). Thus, the two GPI-anchored isoforms Fas2<sup>PB</sup> and Fas2<sup>PC</sup> differentially contribute to the stabilization of the Fas2<sup>TM</sup> gradient on motor axons.

We next asked if the alteration in the Fas2<sup>TM</sup> distribution in the absence of glial Fas2 resulted in glial migration phenotypes. In wild type embryos, peripheral glial nuclei steadily migrate towards the periphery. In all mutants that affect the expression of the Fas2<sup>PB</sup> isoform, final positioning of glial nuclei appeared normal again at the end of migration in stage 16 (Supplementary Figure 4). To test if there are more subtle phenotypes at the onset of migration, we performed *in vivo* live imaging of glial migration of stage 14-16 embryos. Interestingly, in mutants affecting the graded expression of Fas2<sup>TM</sup>, we noted a wiggling of glial nuclei during the short period of cell migration towards the periphery (see table in Figure 4B, and compare tracks in Supplementary Figure 4A,B). Glial cells move backwards towards the CNS for a short period of time before resuming their outwards migration (see white and orange arrow heads in Supplementary Figure 4C-H). We did not note such a phenotype in mutants affecting Fas2<sup>PC</sup> expression. Together, these data argue that the distribution of Fas2, and especially glial Fas2 expression are required for a coordinated and



directed onset of migration. At the same time, mechanisms are in place that allow to overcome these initial phenotypes during subsequent development.

## Discussion

The *Drosophila* NCAM homolog *fasciclin2* (*fas2*) has been first identified as a motor neuron specific protein (Grenningloh et al., 1991). Previously we showed that Fas2 has a broader expression profile and is found in glial and renal cells but no clear analysis of the different Fas2 isoforms was done (Halberg et al., 2016; Silies and Klämbt, 2010). The newly generated Fas2<sup>MiMIC12898::mCherry</sup> allele, which labels all Fas2 isoforms, shows an even broader expression pattern including the tracheal system. Further phenotypic studies revealed a previously unknown tracheal phenotype of *fas2* mutants. In addition, we analyzed isoforms Fas2<sup>PB</sup> and Fas2<sup>PC</sup> and show that they are both tethered to the membrane via a GPI-anchor. We reveal, the distinct expression profiles of the different isoforms, and particularly show that Fas2<sup>PB</sup> is expressed in glial cells. Our data demonstrated functional redundancy of the different isoforms. Finally, rescue experiments demonstrate that Fas2 can act independent of its homophilic adhesion properties.

In the CNS, the GPI-linked isoforms Fas2<sup>PB</sup> and Fas2<sup>PC</sup> are found in non-neuronal cells (glia and trachea) and neurons, whereas the transmembrane linked isoforms are generated exclusively in neurons. A similar expression profile has been noted in mammals. Here, the GPI-linked NCAM form, NCAM120, is expressed predominantly by glial cells whereas the neuronal forms, NCAM180 and NCAM140 are expressed by neurons (Maness and Schachner, 2007). In contrast to mutations in the mammalian *NCAM* gene (Cremer et al., 1994a), mutations in *Drosophila fas2* result in a lethal phenotype (Grenningloh et al., 1991). Here we show that the lethality

associated with *Drosophila* *fas2* mutants, might also not be due to severe motor dysfunction. Instead, our data suggest that it might be due to disrupted tracheal development as we noted defective tracheal inflation in *fas2<sup>EB112</sup>* mutants. Similar phenotypes are caused by mutations that affect the very large extracellular protein Uninflated (Zhang and Ward, 2009) and by mutations affecting the chitin deacetylases Serpentine or Vermiform (Luschnig et al., 2006; Wang et al., 2006). Importantly, here we have only addressed two phenotypic traits, lethality and glial migration but have not studied other functions of *fas2* during the development of the neuromuscular junction or the brush border in Malpighian tubules (Halberg et al., 2016; Kohsaka et al., 2007; Thomas et al., 1997).

Expression of the *fas2* gene is controlled by one promoter suggesting that the differential expression during development is brought about by differential splicing. Such a cell-type specific difference in splicing activity has also been determined for *tramtrack* and *neurexinIV*. Some proteins controlling nervous system specific splicing such as HOW and Crooked Neck have been identified which may also control the neural specific splicing of additional RNAs (Edenfeld et al., 2006; Giesen et al., 1997; Rodrigues et al., 2012).

Deletion mutants affecting expression of all Fas2 isoforms result in late embryonic, or early larval lethality. A small deletion mutant that removed five of the seven isoforms, all of which are transmembrane proteins, is still viable with no discernible phenotype. The same is true for animals generated by reintroducing a truncated *fas2* locus allowing the expression of only one of the seven isoforms, the GPI linked Fas2<sup>PC</sup> protein. A drawback in these mutant and rescue experiments is that we do not know how the splicing pattern is affected by the different mutants. Do glial cells that normally activate *fas2<sup>PB</sup>* expression now also activate *fas2<sup>PC</sup>*? We do not favor this idea since in mutants affecting *fas2<sup>PB</sup>* expression we note a subtle glial migration

phenotype, suggesting that no compensatory Fas2 expression by an altered cell-type specific splicing is induced.

Thus, one might anticipate that the different Fas2 isoforms act in a redundant manner to mediate adhesion. Such an adhesive interaction could even be mediated by a secreted Fas2 protein that after binding to the cell surface via another interactor, might still be able to mediate adhesive cell-cell interactions. Alternatively, Fas2 might be a signaling molecule and could act non-cell autonomously. The results of our cell-type specific rescue experiments are supporting this model. Whereas expression of membrane anchored Fas2 in glial cells does not rescue lethality associated with the *fas2* null phenotype, glial expression of secreted Fas2 is able to rescue the lethal *fas2* phenotype. Based on these findings we postulate that Fas2 has some signaling function perceived by a still unknown receptor to allow survival of the animal.

In hippocampal neurons from mice it was shown that NCAM cannot only mediate homophilic cell-cell interactions but can also trigger exocytosis via the FGF-receptor (Chernyshova et al., 2011). In addition, NCAM is able to bind and hydrolyze extracellular adenosine triphosphate (ATP) which also exerts important signaling functions (Dzhandzhugazyan and Bock, 1997). Similar properties might account for the observed rescuing abilities of the secreted *Drosophila* Fas2 protein.

Alternatively, heterophilic interaction partners could be postulated. For the Fas2 orthologue NCAM such heterophilic interaction partners have been described already, including the Ig-domain cell adhesion molecules L1 and TAG-1 and signaling receptors such as FGF-receptor and the GDNF and GDNF family receptor  $\alpha$  (Kiselyov, 2008; Kiselyov et al., 2003; Maness and Schachner, 2007; Paratcha et al., 2003). Heterophilic interaction partners are also known for the *Drosophila* Fas2 protein. All Fas2 isoforms share a common extracellular domain comprising 5 Ig-

domains and 2 fibronectin type III domains, with only isoform Fas2<sup>PF</sup> being distinct by a small exon coding for just 15 amino acids that are added to the N-terminal first Ig-domain. Genome-wide interaction studies have demonstrated that the extracellular domain of Fas2 shows homophilic interactions and also binds additional Ig-domain proteins (*CG33543* and *CG15630* or *factor of interpulse interval, fipi*) (Özkan et al., 2013). We do not favor a role of *CG33543* and *fipi* as crucial Fas2 receptors, since both proteins which carry three Ig-domains and one fibronectin type three domain lack a discernible membrane-anchor and are thus likely secreted proteins. Although *CG15630* expression shows some overlap with Fas2 expression (Supplementary Figure 5), two mutator piggyback transposon insertions in the first coding intron, causing translational stops in all orientations, are homozygous viable (Schuldiner et al., 2008). Likewise, a CRISPR/Cas9-induced *CG33543* null mutant that we generated is homozygous viable. Therefore, additional interaction partners will need to be identified.

## Materials and Methods

### Genetics

Flies were raised at 25°C according to standard procedures. Rescue and gain-of-function studies were carried out using the Gal4/UAS system (Brand and Perrimon, 1993). The following fly strains were used: *fas2*<sup>EB112</sup> (Grenningloh et al., 1991); *Fas2*<sup>CB03613</sup>; *Fas2*<sup>GFP397</sup>; *Fas2*<sup>GFP778</sup> (Halberg et al., 2016; Silies and Klämbt, 2010); *PBac{602.P.SVS.-1}Fas2*<sup>CPTI000483</sup> (Kyoto DGRC# 115501); *PBac{681.P.FSVS.-1}Fas2*<sup>CPTI001279</sup> (Kyoto DGRC# 115144); *Mi{MIC}Fas2*<sup>MI12989</sup> (BDSC# 58577); *Mi{MIC}fipi*<sup>MI06000</sup> (BDSC# 43778); *Dp(1;3)DC075* (BDSC# 30247); *Dp(1;3)DC115* (BDSC# 31445); *Dp(1;3)DC465* (BDSC# 32299); *nsyb-Gal4*, *elav-GAL4* (Luo et al.,

1994); *repo-GAL4* (BDSC#7415); *repo4.3-GAL4* (Lee and Jones, 2005); *P{UAS-Stinger}2* (BDSC# 65402); *y1 P(nos-cas9, w+) M(3xP3-RFP.attP)ZH-2A w\** (Port et al., 2014). Transgenes were generated using  $\phi$ C31-based transformation in the landing site *86Fb* using standard protocols (Bischof et al., 2007). The *Dp(1;3)Fas2* was inserted in landing site *VK33* by BestGene Inc.

The following strains were generated in this study: The deletion alleles *Df(1)fas2* and *Df(1)fas2<sup>ΔTM</sup>* were generated via FRT/Flp-mediated recombination using *{XP}d07035* and PBac *{WH}f06654* or PBac *{PB}c04606*, respectively (Exelixis collection at Harvard Medical School; (Parks et al., 2004)) (see also Figure 3). In *Df(1)fas2* approximately 75 kb of the *fas2* gene locus, including the 5' UTR, coding exons, 3' UTR and the neighboring gene *GlcAT-I* are deleted. In *Df(1)fas2<sup>ΔTM</sup>* approximately 7 kb of the *fas2* 3' end, including exons coding for *fas2<sup>TM</sup>*, the *fas2* 3' UTR and *GlcAT-I* were flipped out. Both deletions were verified by loss of *white* expression and/or PCR using the following primers: XP5' hybrid AATGATTCGCAGTGGGAAGGCT, WH5' hybrid GACGCATGATTATCTTTTACGTGAC (Parks et al., 2004).

*Fas2<sup>MI12989::mCherry</sup>* and *Fipi<sup>MI06000::mCherry</sup>* were generated according to standard protocols using the vector pBS-KS-attB1-2-PT-SA-SD-1-mCherry (DGRC# 1307) (Venken et al., 2011).

The following crosses were performed for neuronal rescue experiments:

*fas2<sup>EB112</sup>/FM7*; *UAS-fas2<sup>PD-YFP</sup>* / *UAS-fas2<sup>PD-YFP</sup>* X *w<sup>1118</sup>/FM7*; *nsyb-Gal4*. For glial rescue experiments we used: *fas2<sup>EB112</sup>/FM7*; *UAS-fas2<sup>extra-YFP</sup>* / *CyO* X *w<sup>1118</sup>* / *FM7*; *repo-Gal4/repo-Gal4*; *repo-Gal4/TM6*. More than 500 F1 flies were analyzed for each cross. Phenotypic rescue was noted when males appeared that carried a mutant *fas2* X-chromosome, which normally results in lethality. The same principle accounts for mutant *fas2* rescue experiments using molecularly defined chromosomal duplications. The following crosses were performed to test the genetic requirements

of *fas2*: *fas2<sup>EB112</sup>/FM7* virgins were crossed to *Dp(1;3)DC075*; *Dp(1;3)DC115*; *Dp(1;3)DC465*; *Dp(1;3)Fas2* and *w<sup>1118</sup>* males. Percentage of eclosed *fas2* males and F1 flies analyzed are stated in brackets for each duplication used: *Dp(1;3)DC075* (10% *fas2* males eclosed, F1 200 flies), *Dp(1;3)DC115* (40% *fas2* males eclosed, F1 450 flies), *Dp(1;3)DC465* (55% *fas2* males eclosed, F1 420 flies), *Dp(1;3)Fas2* (52% *fas2* males eclosed, F1 650 flies), and *w<sup>1118</sup>* (3% *fas2* males eclosed, F1 160 flies).

### Generation of CRISPR *fas2* Isoform-specific mutants

CRISPR/Cas9 based manipulations were done as described (Bassett et al., 2013; Port et al., 2014; Port et al., 2015). sgRNAs were designed using CRISPR Optimal Target Finder with a guide length of 16-20 nt, the stringency set to “high”, and “NGG only” for PAM site identification (Gratz et al., 2014). Chosen sgRNA had no predicted off-targets. Target sequences for isoform specific *fas2* mutants: *fas2<sup>PB</sup>* ggtgcagcgcactctgtgcaGGG and *fas2<sup>PC</sup>* gggtcagctaataacaatctCGG are upstream of the potential GPI anchor or predicted transmembrane domain, respectively (see Supplementary Figure 6 for details). Targeting sgRNAs were produced by *in vitro* transcription using the Megascript T7 Kit (Ambion) and injected into *nos-Cas9* (X) flies. In *fas2<sup>ΔPB</sup>*, a 28bp deletion caused a frame shift and introduced an early translational stop after three amino acids, truncating the original Fas2<sup>PB</sup> protein sequence after 741 amino acids. Both putative GPI anchor sites (amino acid 742 and 744) were deleted. In *fas2<sup>ΔPC</sup>*, a five bp deletion introduced a premature translational stop after eight amino acids, truncating the original Fas2<sup>PC</sup> protein sequence after 742 amino acids.

Generation of *fas2<sup>ΔPB, ΔTM</sup>* double mutant: Target sequences *fas2<sup>TM U6.3</sup>* tgctgcatcaccgtccacatGGG and *fas2<sup>PB U6.1</sup>* aatccccatcctcgacgagTGG were cloned into pCFD4 plasmid and inserted in the insertion site *attP86Fb<sup>RFP-</sup>* on the third

chromosome. Target sequence for mutating *fas2<sup>TM</sup>* was expressed under the *U6:3* promoter, whereas target sequence and the gRNA core sequence for *fas2<sup>PB</sup>* was expressed under the *U6:1* promoter. *nos-cas9* flies were crossed to the resulting transgene to induce CRISPR/Cas9-mediated mutations. Sequencing of PCR products of the targeted sites revealed that one bp was deleted at the target site *fas2<sup>TM</sup><sup>U6.3</sup>* and 14 bp were deleted and an additional nine bp were inserted at the target site *fas2<sup>PB</sup><sup>U6.1</sup>*. Both mutations induced a frameshift and resulted in a termination of the *Fas2<sup>TM</sup>* protein translation after additional 30, and nine amino acids for the *Fas2<sup>PB</sup>* isoform, respectively. Induced mutations in the allele *fas2<sup>ΔPB, ΔTM</sup>*, *fas2* truncated the original *Fas2<sup>TM</sup>* protein sequence after 777 amino acids and the original *Fas2<sup>PB</sup>* protein sequence after 742 amino acids. The *Fas2<sup>PB</sup>* isoform lost the GPI-anchoring and the *Fas2<sup>TM</sup>* lost part of the transmembrane domain and the entire intracellular domain. The transmembrane domain is predicted to be encoded by amino acids 759-781. The major putative GPI anchor site is localized at the serine at amino acid 744. Homozygous flies for *fas2<sup>ΔPB, ΔTM</sup>* alleles were viable, fertile and expression of the isoform *Fas2<sup>TM</sup>* specific mAb 1D4 epitope is absent from all homozygous tissues tested, confirming the loss of all isoforms carrying the cytoplasmic domain.

Generation of *fas2<sup>ΔTM</sup>* and *fas2<sup>ΔPB</sup>* in a *fas2<sup>GFP397</sup>* background: Transgenic animals expressing a gRNA construct targeting *Fas2<sup>TM</sup>* (target site: aggaattgacgtcatccaagTGG) or *Fas2<sup>PB</sup>* (target site: aatccccatccctcgacgacTGG) were cloned into pCFD3-U6:3 and integrated into the landing site *attP86Fb<sup>RFP</sup>* (Bischof et al., 2007) in a *fas2<sup>GFP397</sup>* background. To introduce CRISPR-induced mutations, *fas2<sup>GFP397</sup>; ;pCFD3-U6:3fas2<sup>TM</sup>* and *fas2<sup>GFP397</sup>; ;pCFD3-U6:3fas2<sup>PB</sup>* transgenic males were crossed to *nos-Cas9* (X) virgin flies. *fas2<sup>GFP397</sup>*, *fas2<sup>ΔTM</sup>*: A six bp deletion and a one bp insertion induced a premature translational stop of the *Fas2<sup>TM</sup>* protein after

two amino acids. The *fas2<sup>ΔTM</sup>* allele results in a truncated protein after 740 amino acids, deleting the transmembrane domain and the cytoplasmic domains of Fas2<sup>TM</sup>. *fas2<sup>GFP397</sup>*, *fas2<sup>ΔPB</sup>*: A two bp deletion induced a frameshift and a delayed translational stop of the Fas2<sup>PB</sup> protein after thirteen amino acids. The mutation results in the loss of Fas2<sup>PB</sup> GPI anchoring to the membrane and an after 742 amino acids truncated, potentially secreted protein version. Effects on Fas2<sup>TM</sup> expression were confirmed by 1D4 epitope expression in *fas2<sup>ΔTM</sup>* or *fas2<sup>ΔPB</sup>* homozygous flies.

## Molecular Biology

### Cloning of Fas2<sup>PC</sup> expression tools

pBS-KS-attB1-2-SV40-FRT backbone vector: pUAST-attB-rfA was used as template to amplify SV40 with corresponding primer PstI\_SV40\_for (agtctgcaggatctttgtgaaggaacct) and SV40\_EcoRI\_rev (CGCAGAATTCggatccagacatgataagat) introducing *PstI* and *EcoRI* restriction sites. PstI-SV40-EcoRI PCR product was digested with *PstI/EcoRI* and purified using column purification (Quiagen). *PstI/EcoRI* digested SV40 PCR product was ligated into *PstI/EcoRI* cleaved pBS-KS-attB1-2-FRT vector.

pBS-KS-attB1-2\_ fas2<sup>PC::V5</sup>\_ fas2<sup>PB::HA</sup>\_SV40\_FRT\_white: V5 and HA tags were introduced using RF (restriction free) cloning. *BsaI* restriction sites were added to the different fragments (fragment 1: fas2<sup>PB::HA</sup>, fragment 2: fas2<sup>PC::V5</sup>) during amplification from *w<sup>1118</sup>* gDNA. *BsaI* digested fragments 1+2 were ligated in one reaction into the *XbaI/SpeI* digested backbone vector pBS-KS-attB1-2-SV40-FRT. Primer used for RF cloning: RF\_cloning\_Fas2PC::V5\_for (CCACCACAATAAGCATAACACTTAGTGTCTAGCCTCAATGTTAGCCggaGG



TAAGCCTATCCCTAACCCCTCTCCTCGG), RF\_cloning\_Fas2PC::V5\_rev  
(tgtcacaccacagaagtaaggttccttcacaaagatccctgcagactagttatccCGTAGAATCGAGACC  
GAGGAGAGGGTTAGGG), RF\_cloning\_Fas2PB::HA\_for  
(TATCGAAAATCGACAACCAATATCGAAAAAACCAACAGATAATCCCCATggaTA  
CCCATACGATGTTCCAGATTA), RF\_cloning\_Fas2PB::HA\_rev  
(GTGAAAATTACAAGCAGTTGGGCCAGGGGTGCAGCGCCACTCGTCGAGGGtcc  
AGCGTAATCTGGAACATCGTATG). Primer used to amplify fragments 1 and 2, and  
to clone into pENTR, introducing *Bsal* restriction sites and leaving *Xba*I (for Fragment  
2), and *Spe*I (for Fragment 1) overhangs for subsequent cloning:

Bsal\_XbaI\_MI12989\_Fas2PC\_for\_1

(CACCGgtctctctagACCTAGCTCAGGAATTTGTT), MI12989\_Fas2PC\_Bsal\_rev\_1

(ggtctcaTTAGGCTAACATTGAGGCTA), Bsal\_MI\_Fas2RC\_RNA\_for\_2

(CACCGgtctcaCTAAGCATTACAATTCGTTC), MI\_Fas2PB\_SpeI\_Bsal\_rev\_2

(ggtctcactagTTAAGCAGTGTGCGTCGTCG). At the end, PCR amplified *white*

marker was introduced into all of the plasmids via *Xho*I/*Hind*III digest. All plasmids

were injected into *Mi{MIC}Fas2<sup>MI12989</sup>* (BDSC# 58577) flies to generate transgenes.

### Generation of Fas2 constructs

UAS constructs of *fas2<sup>PB</sup>* and *fas2<sup>PC</sup>* CDS were generated using standard  
procedures, *w<sup>118</sup>* embryonic cDNA as template, and a pUAST-attB-rfA plasmid as  
destination vector. Primers used for cloning: TOPO *fas2* Exon1 for

caccATGGGTGAATTGCCGCCAAA and *fas2* PB cDNA rev

TTAAGCAGTGTGCGTCGTCG or *fas2* PC cDNA rev TTAGGCTAACATTGAGGCTA

respectively. Site-directed mutagenesis (NEB) was used to introduce a single HA tag

(GGYPYDVPDYAGG, with two adjacent glycins as spacers (underlined)) at position

+100bp of the *fas2<sup>PB</sup>* and *fas2<sup>PC</sup>* CDS, directly after the endogenous signal peptide sequence (*UAS-fas2<sup>HA-PB</sup>* and *UAS-fas2<sup>HA-PC</sup>*). Primers used for site-directed mutagenesis: *fas2<sup>HA</sup>* for:

CTCTGCAGCTGCTCTTTAATAGAACTGACCCGTGCGCAGTCCCCCATCCTGggag  
gaTACCCATACGATGTTCCAGATTAC and *fas2<sup>HA</sup>* rev:

CATACGATGTTCCAGATTACGCTggaggaGAGATTTATCCCAAACAAGAAGTCCAG  
CGCAAGCCAGTGGGCAAGCCCCTG.

### **RNA extraction and RT-PCR**

RNA was isolated from *w<sup>1118</sup>* embryos (all stages) using TRIsure™ (Bioline) and RT-PCR was performed using SuperScript™ II Reverse Transcriptase (Invitrogen)

according to manufacturer's guidelines. Oligonucleotides used for detection of *fas2* splice-variants: Fas2 A for CTGAGCGACAGGTCTTCTCC, Fas2 A rev

GCCGAATTCTTCCCGATTAT, Fas2 A PEST rev CGGTGGCTCCTTTACCAG, Fas2 Exon6 for CAGATTGCGCGTACATTGTG, Fas2 B rev

CAAATCAGCAGCATTGTGCG, Fas2 C rev TGTGGCTGTTGTTGTTGTTG, Fas2 F for CGATCCACTGTATGATTCCAAG, Fas2 F rev GTGGCATCTCGAATCCAAC,

Fas2-RG for TTTACGGTTGGCGTTTTCCG, Fas2-RH rev CCGCGCATAAACCCAATTGT.

### **Immunohistochemistry and live imaging**

Fixation and preparation of tissues for immunohistochemistry was performed as described previously (Yuva-Aydemir et al., 2011). Antibodies used were mouse anti-Repo (1:5), mouse anti-Fas2 (1:5) (all DSHB); rabbit anti-GFP (1:1000; Invitrogen); anti-dsRed and goat anti-HRP-DyLight™ 647 conjugated (1:1000, Dianova).

Secondary antibodies used in this study were: goat anti-mouse IgG and goat anti-rabbit IgG with the fluorophore conjugates Alexa Fluor-488, -568 and -647 (1:1000; Molecular Probes). Specimen were analyzed using a Zeiss LSM710 or LSM880. Live imaging analysis was performed using a *UltraView RS*, Perkin Elmer or a Zeiss LSM 5 Duo microscope. Original confocal data, images, orthogonal sections, and movie sequences were processed using the Zeiss ZEN 2012 software (Zeiss), Adobe Photoshop CS6, and Fiji (Schindelin et al., 2012). The chorion of staged embryos was removed by 50% NaCl treatment for 3 min. Embryos were aligned on heptane coated coverslips in glass bottom dishes (MatTek Corp.) and imaged covered in 10S Voltalef oil to prevent drying of embryos. Glial cell migration was recorded with a speed of 1 stack/min over 120-180 min. At least 9 and up to 30 embryos were imaged for each genotype.

### **Cell Movement Analysis**

Manual tracking of glial cell migration was performed using Fiji (*control*: n=4 embryos, *fas2<sup>EB112</sup>*: n=7 embryos; 30-40 individual glial cell nuclei were tracked per movie). In order to quantify aberrant cell movements, we implemented a custom Matlab script. First, we extracted the movement direction using consecutive positional tracking estimates of the nuclei. As shown in Supplementary Figure 4I the movement is characterized by multiple cell clusters migrating on parallel lines from a common starting line (line A in Supplementary Figure 4I) to a shared destination line (line B in Supplementary Figure 4I). Using the direction of a vector orthogonal to these lines as the standard movement direction (i.e. the mode direction), we then quantified nuclei motion by counting the number of frames in which the movement direction deviates more than  $\pm 90^\circ$  of this mode direction (i.e. moving in the opposite direction of the mode; cf. Supplementary Figure 4J). By incrementing a counter every time a

misdirection movement event (MME) is detected we can plot the length of the MMEs against the overall count of frames with misdirected movement (Supplementary Figure 4K).

### **Statistical analysis of Fas2 intensity ratio**

Statistical analysis of Fas2 intensity ratio was done as published (Silies and Klämbt, 2010). In short: To quantify Fas2 expression, two regions of interest close to the CNS-PNS transition zone and in a distal region of the nerve behind the growth cone were defined and the mean intensity was determined using ImageJ software (NIH). Fas2 expression in nerves of 2-6 hemisegments per embryo was measured. The mean of Fas2 intensity ratio per embryo was used for subsequent statistical analysis using the Mann-Whitney Rank Sum test.

### **Biochemical methods**

UAS-*fas2<sup>PB</sup>* and UAS-*fas2<sup>PC</sup>* constructs were transfected in S2 R+ cells (Stork et al., 2009). After 2 days, cells were incubated for 1 h at 25°C with serum free medium, or serum free medium containing Phosphatidylinositol-specific phospholipase C (PiPLC, Sigma-Aldrich, Cat #P5542) (1U/ml) as described (Petri et al., 2019). Isolated proteins from cell-lysates and supernatant were analyzed by western blot.

## **Acknowledgments**

We are thankful to all members of the Klämbt lab for help throughout the project and comments on the manuscript. J. Börgers for help during the generation of the mCherry conversion of the *fas2* MiMIC insertion, F. Port for sharing of CRISPR reagents and much advice. Work in the Klämbt lab is supported through a grant of the DFG (SFB 1348 B5).

## References

- Bassett, A. R., Tibbit, C., Ponting, C. P. and Liu, J.-L.** (2013). Highly efficient targeted mutagenesis of *Drosophila* with the CRISPR/Cas9 system. *Cell Rep* **4**, 220–228.
- Bieber, A. J., Snow, P. M., Hortsch, M., Patel, N. H., Jacobs, J. R., Traquina, Z. R., Schilling, J. and Goodman, C. S.** (1989). *Drosophila* neuroglian: a member of the immunoglobulin superfamily with extensive homology to the vertebrate neural adhesion molecule L1. *Cell* **59**, 447–460.
- Bischof, J., Maeda, R. K., Hediger, M., Karch, F. and Basler, K.** (2007). An optimized transgenesis system for *Drosophila* using germ-line-specific phiC31 integrases. *Proc Natl Acad Sci USA* **104**, 3312–3317.
- Brand, A. H. and Perrimon, N.** (1993). Targeted gene expression as a means of altering cell fates and generating dominant phenotypes. *Development* **118**, 401–415.
- Buszczak, M., Paterno, S., Lighthouse, D., Bachman, J., Planck, J., Owen, S., Skora, A. D., Nystul, T. G., Ohlstein, B., Allen, A., et al.** (2007). The carnegie protein trap library: a versatile tool for *Drosophila* developmental studies. *Genetics* **175**, 1505–1531.
- Chen, W. and Hing, H.** (2008). The L1-CAM, Neuroglian, functions in glial cells for *Drosophila* antennal lobe development. *Devel Neurobio* **68**, 1029–1045.
- Chernyshova, Y., Leshchyn'ska, I., Hsu, S.-C., Schachner, M. and Sytnyk, V.** (2011). The neural cell adhesion molecule promotes FGFR-dependent phosphorylation and membrane targeting of the exocyst complex to induce exocytosis in growth cones. *Journal of Neuroscience* **31**, 3522–3535.
- Cremer, H., Lange, R., Christoph, A., Plomann, M., Vopper, G., Roes, J., Brown, R., Baldwin, S., Kraemer, P. and Scheff, S.** (1994a). Inactivation of the N-CAM gene in mice results in size reduction of the olfactory bulb and deficits in spatial learning. *Nature* **367**, 455–459.
- Cremer, H., Lange, R., Christoph, A., Plomann, M., Vopper, G., Roes, J., Brown, R., Baldwin, S., Kraemer, P., Scheff, S., et al.** (1994b). Inactivation of the N-CAM gene in mice results in size reduction of the olfactory bulb and deficits in spatial learning. *Nature* **367**, 455–459.
- Davis, G. W., Schuster, C. M. and Goodman, C. S.** (1997). Genetic analysis of the mechanisms controlling target selection: target-derived Fasciclin II regulates the pattern of synapse formation. *Neuron* **19**, 561–573.
- Dzhandzhugazyan, K. and Bock, E.** (1997). Demonstration of an extracellular ATP-binding site in NCAM: functional implications of nucleotide binding. *Biochemistry* **36**, 15381–15395.

- Edenfeld, G., Volohonsky, G., Krukkert, K., Naffin, E., Lammel, U., Grimm, A., Engelen, D., Reuveny, A., Volk, T. and Klämbt, C.** (2006). The splicing factor crooked neck associates with the RNA-binding protein HOW to control glial cell maturation in *Drosophila*. *Neuron* **52**, 969–980.
- Eichler, K., Li, F., Litwin-Kumar, A., Park, Y., Andrade, I., Schneider-Mizell, C. M., Saumweber, T., Huser, A., Eschbach, C., Gerber, B., et al.** (2017). The complete connectome of a learning and memory centre in an insect brain. *Nature Publishing Group* **548**, 175–182.
- Fankhauser, N. and Mäser, P.** (2005). Identification of GPI anchor attachment signals by a Kohonen self-organizing map. *Bioinformatics* **21**, 1846–1852.
- Fremion, F., Darboux, I., Diano, M., Hipeau-Jacquotte, R., Seeger, M. A. and Piovant, M.** (2000). Amalgam is a ligand for the transmembrane receptor neurotactin and is required for neurotactin-mediated cell adhesion and axon fasciculation in *Drosophila*. *EMBO J* **19**, 4463–4472.
- Giesen, K., Hummel, T., Stollewerk, A., Harrison, S., Travers, A. and Klämbt, C.** (1997). Glial development in the *Drosophila* CNS requires concomitant activation of glial and repression of neuronal differentiation genes. *Development* **124**, 2307–2316.
- Gratz, S. J., Ukken, F. P., Rubinstein, C. D., Thiede, G., Donohue, L. K., Cummings, A. M. and O'Connor-Giles, K. M.** (2014). Highly specific and efficient CRISPR/Cas9-catalyzed homology-directed repair in *Drosophila*. *Genetics* **196**, 961–971.
- Grenningloh, G., Rehm, E. J. and Goodman, C. S.** (1991). Genetic analysis of growth cone guidance in *Drosophila*: fasciclin II functions as a neuronal recognition molecule. *Cell* **67**, 45–57.
- Gundersen, V., Storm-Mathisen, J. and Bergersen, L. H.** (2015). Neuroglial Transmission. *Physiol. Rev.* **95**, 695–726.
- Halberg, K. A., Rainey, S. M., Veland, I. R., Neuert, H., Dornan, A. J., Klämbt, C., Davies, S.-A. and Dow, J. A. T.** (2016). The cell adhesion molecule Fasciclin2 regulates brush border length and organization in *Drosophila* renal tubules. *Nat Commun* **7**, 11266.
- Heinz, D. W., Essen, L.-O. and Williams, R. L.** (1998). Structural and mechanistic comparison of prokaryotic and eukaryotic phosphoinositide-specific phospholipases C. - PubMed - NCBI. *Journal of Molecular Biology* **275**, 635–650.
- Higgins, M. R., Gibson, N. J., Eckholdt, P. A., Nighorn, A., Copenhaver, P. F., Nardi, J. and Tolbert, L. P.** (2002). Different isoforms of fasciclin II are expressed by a subset of developing olfactory receptor neurons and by olfactory-nerve glial cells during formation of glomeruli in the moth *Manduca sexta*. *Developmental Biology* **244**, 134–154.
- Hortsch, M., Bieber, A. J., Patel, N. H. and Goodman, C. S.** (1990). Differential splicing generates a nervous system-specific form of *Drosophila* neuroglian. *Neuron* **4**, 697–709.

- Hosoya, T., Takizawa, K., Nitta, K. and Hotta, Y.** (1995). glial cells missing: a binary switch between neuronal and glial determination in *Drosophila*. *Cell* **82**, 1025–1036.
- Jones, B. W., Fetter, R. D., Tear, G. and Goodman, C. S.** (1995). glial cells missing: a genetic switch that controls glial versus neuronal fate. *Cell* **82**, 1013–1023.
- Kammerer, M. and Giangrande, A.** (2001). Glide2, a second glial promoting factor in *Drosophila melanogaster*. *EMBO J* **20**, 4664–4673.
- Kim, B.-T., Tsuchida, K., Lincecum, J., Kitagawa, H., Bernfield, M. and Sugahara, K.** (2003). Identification and characterization of three *Drosophila melanogaster* glucuronyltransferases responsible for the synthesis of the conserved glycosaminoglycan-protein linkage region of proteoglycans. Two novel homologs exhibit broad specificity toward oligosaccharides from proteoglycans, glycoproteins, and glycosphingolipids. *J Biol Chem* **278**, 9116–9124.
- Kiselyov, V. V.** (2008). WITHDRAWN: NCAM and the FGF-Receptor. *Neurochem. Res.* **23**, 879.
- Kiselyov, V. V., Skladchikova, G., Hinsby, A. M., Jensen, P. H., Kulahin, N., Soroka, V., Pedersen, N., Tsetlin, V., Poulsen, F. M., Berezin, V., et al.** (2003). Structural basis for a direct interaction between FGFR1 and NCAM and evidence for a regulatory role of ATP. *Structure* **11**, 691–701.
- Kohsaka, H., Takasu, E. and Nose, A.** (2007). In vivo induction of postsynaptic molecular assembly by the cell adhesion molecule Fasciclin2. *The Journal of Cell Biology* **179**, 1289–1300.
- Kristiansen, L. and Hortsch, M.** (2008). Fasciclin II: The NCAM Ortholog in *Drosophila melanogaster*.
- Larderet, I., Fritsch, P. M., Gendre, N., Neagu-Maier, G. L., Fetter, R. D., Schneider-Mizell, C. M., Truman, J. W., Zlatic, M., Cardona, A. and Sprecher, S. G.** (2017). Organization of the *Drosophila* larval visual circuit. *eLife Sciences* **6**, e28387.
- Lee, B. P. and Jones, B. W.** (2005). Transcriptional regulation of the *Drosophila* glial gene repo. *Mechanisms of Development* **122**, 849–862.
- Liebl, E. C., Rowe, R. G., Forsthoefel, D. J., Stammler, A. L., Schmidt, E. R., Turski, M. and Seeger, M. A.** (2003). Interactions between the secreted protein Amalgam, its transmembrane receptor Neurotactin and the Abelson tyrosine kinase affect axon pathfinding. *Development* **130**, 3217–3226.
- Lowe, N., Rees, J. S., Roote, J., Ryder, E., Armean, I. M., Johnson, G., Drummond, E., Spriggs, H., Drummond, J., Magbanua, J. P., et al.** (2014). Analysis of the expression patterns, subcellular localisations and interaction partners of *Drosophila* proteins using a pigP protein trap library. *Development* **141**, 3994–4005.



- Luo, L., Liao, Y. J., Jan, L. Y. and Jan, Y. N.** (1994). Distinct morphogenetic functions of similar small GTPases: *Drosophila* Drac1 is involved in axonal outgrowth and myoblast fusion. *Genes & Development* **8**, 1787–1802.
- Luschnig, S., Bätz, T., Armbruster, K. and Krasnow, M. A.** (2006). serpentine and vermiform encode matrix proteins with chitin binding and deacetylation domains that limit tracheal tube length in *Drosophila*. *Curr Biol* **16**, 186–194.
- Maness, P. F. and Schachner, M.** (2007). Neural recognition molecules of the immunoglobulin superfamily: signaling transducers of axon guidance and neuronal migration. *Nat Neurosci* **10**, 19–26.
- Nagarkar-Jaiswal, S., Lee, P.-T., Campbell, M. E., Chen, K., Anguiano-Zarate, S., Gutierrez, M. C., Busby, T., Lin, W.-W., He, Y., Schulze, K. L., et al.** (2015). A library of MiMICs allows tagging of genes and reversible, spatial and temporal knockdown of proteins in *Drosophila*. *eLife Sciences* **4**, e05338.
- Noordermeer, J. N., Kopczynski, C. C., Fetter, R. D., Bland, K. S., Chen, W. Y. and Goodman, C. S.** (1998). Wrapper, a novel member of the Ig superfamily, is expressed by midline glia and is required for them to ensheath commissural axons in *Drosophila*. *Neuron* **21**, 991–1001.
- Özkan, E., Carrillo, R. A., Eastman, C. L., Weiszmann, R., Waghray, D., Johnson, K. G., Zinn, K., Celniker, S. E. and Garcia, K. C.** (2013). An extracellular interactome of immunoglobulin and LRR proteins reveals receptor-ligand networks. *Cell* **154**, 228–239.
- Paratcha, G., Ledda, F. and Ibáñez, C. F.** (2003). The neural cell adhesion molecule NCAM is an alternative signaling receptor for GDNF family ligands. *Cell* **113**, 867–879.
- Parks, A. L., Cook, K. R., Belvin, M., Dompe, N. A., Fawcett, R., Huppert, K., Tan, L. R., Winter, C. G., Bogart, K. P., Deal, J. E., et al.** (2004). Systematic generation of high-resolution deletion coverage of the *Drosophila melanogaster* genome. *Nat Genet* **36**, 288–292.
- Petri, J., Syed, M. H., Rey, S. and Klämbt, C.** (2019). Non-Cell-Autonomous Function of the GPI-Anchored Protein Undicht during Septate Junction Assembly. *Cell Rep* **26**, 1641–1653.e4.
- Port, F., Chen, H.-M., Lee, T. and Bullock, S. L.** (2014). Optimized CRISPR/Cas tools for efficient germline and somatic genome engineering in *Drosophila*. *Proceedings of the National Academy of Sciences* **111**, E2967–76.
- Port, F., Muschalik, N. and Bullock, S. L.** (2015). Systematic Evaluation of *Drosophila* CRISPR Tools Reveals Safe and Robust Alternatives to Autonomous Gene Drives in Basic Research. *G3 (Bethesda)* **5**, 1493–1502.
- Rodrigues, F., Thuma, L. and Klämbt, C.** (2012). The regulation of glial-specific splicing of Neurexin IV requires HOW and Cdk12 activity. *Development* **139**, 1765–1776.

- Schindelin, J., Arganda-Carreras, I., Frise, E., Kaynig, V., Longair, M., Pietzsch, T., Preibisch, S., Rueden, C., Saalfeld, S., Schmid, B., et al. (2012).** Fiji: an open-source platform for biological-image analysis. *Nat Meth* **9**, 676–682.
- Schneider-Mizell, C. M., Gerhard, S., Longair, M., Kazimiers, T., Li, F., Zwart, M. F., Champion, A., Midgley, F. M., Fetter, R. D., Saalfeld, S., et al. (2016).** Quantitative neuroanatomy for connectomics in *Drosophila*. *eLife Sciences* **5**, e12059.
- Schuldiner, O., Berdnik, D., Levy, J. M., Wu, J. S., Luginbuhl, D., Gontang, A. C. and Luo, L. (2008).** piggyBac-based mosaic screen identifies a postmitotic function for cohesin in regulating developmental axon pruning. *Developmental Cell* **14**, 227–238.
- Schuster, C. M., Davis, G. W., Fetter, R. D. and Goodman, C. S. (1996a).** Genetic dissection of structural and functional components of synaptic plasticity. I. Fasciclin II controls synaptic stabilization and growth. *Neuron* **17**, 641–654.
- Schuster, C. M., Davis, G. W., Fetter, R. D. and Goodman, C. S. (1996b).** Genetic dissection of structural and functional components of synaptic plasticity. II. Fasciclin II controls presynaptic structural plasticity. *Neuron* **17**, 655–667.
- Silies, M. and Klämbt, C. (2010).** APC/C(Fzr/Cdh1)-dependent regulation of cell adhesion controls glial migration in the *Drosophila* PNS. *Nat Neurosci* **13**, 1357–1364.
- Silies, M. and Klämbt, C. (2011).** Adhesion and signaling between neurons and glial cells in *Drosophila*. *Curr Opin Neurobiol* **21**, 11–16.
- Sivachenko, A., Li, Y., Abruzzi, K. C. and Rosbash, M. (2013).** The transcription factor Mef2 links the *Drosophila* core clock to Fas2, neuronal morphology, and circadian behavior. *Neuron* **79**, 281–292.
- Stork, T., Thomas, S., Rodrigues, F., Silies, M., Naffin, E., Wenderdel, S. and Klämbt, C. (2009).** *Drosophila* Neurexin IV stabilizes neuron-glia interactions at the CNS midline by binding to Wrapper. *Development* **136**, 1251–1261.
- Thomas, U., Kim, E., Kuhlendahl, S., Koh, Y. H., Gundelfinger, E. D., Sheng, M., Garner, C. C. and Budnik, V. (1997).** Synaptic clustering of the cell adhesion molecule fasciclin II by discs-large and its role in the regulation of presynaptic structure. *Neuron* **19**, 787–799.
- Venken, K. J. T., Popodi, E., Holtzman, S. L., Schulze, K. L., Park, S., Carlson, J. W., Hoskins, R. A., Bellen, H. J. and Kaufman, T. C. (2010).** A molecularly defined duplication set for the X chromosome of *Drosophila melanogaster*. *Genetics* **186**, 1111–1125.
- Venken, K. J. T., Schulze, K. L., Haelterman, N. A., Pan, H., He, Y., Evans-Holm, M., Carlson, J. W., Levis, R. W., Spradling, A. C., Hoskins, R. A., et al. (2011).** MiMIC: a highly versatile transposon insertion resource for engineering *Drosophila melanogaster* genes. *Nat Meth* **8**, 737–743.

- Vincent, S., Vonesch, J. L. and Giangrande, A.** (1996). Glide directs glial fate commitment and cell fate switch between neurones and glia. *Development* **122**, 131–139.
- Wang, S., Jayaram, S. A., Hemphälä, J., Senti, K.-A., Tsarouhas, V., Jin, H. and Samakovlis, C.** (2006). Septate-junction-dependent luminal deposition of chitin deacetylases restricts tube elongation in the *Drosophila* trachea. *Curr Biol* **16**, 180–185.
- Wheeler, S. R., Banerjee, S., Blauth, K., Rogers, S. L., Bhat, M. A. and Crews, S. T.** (2009). Neurexin IV and Wrapper interactions mediate *Drosophila* midline glial migration and axonal ensheathment. *Development* **136**, 1147–1157.
- Wright, J. W. and Copenhaver, P. F.** (2001). Cell type-specific expression of fasciclin II isoforms reveals neuronal-glial interactions during peripheral nerve growth. *Developmental Biology* **234**, 24–41.
- Yamamoto, M., Ueda, R., Takahashi, K., Saigo, K. and Uemura, T.** (2006). Control of axonal sprouting and dendrite branching by the Nrg-Ank complex at the neuron-glia interface. *Curr Biol* **16**, 1678–1683.
- Yildirim, K., Petri, J., Kottmeier, R. and Klämbt, C.** (2018). *Drosophila* glia: Few cell types and many conserved functions. *Glia* **21**, 276.
- Yuva-Aydemir, Y., Bauke, A.-C. and Klämbt, C.** (2011). Spinster Controls Dpp Signaling during Glial Migration in the *Drosophila* Eye. *Journal of Neuroscience* **31**, 7005–7015.
- Zeev-Ben-Mordehai, T., Mylonas, E., Paz, A., Peleg, Y., Toker, L., Silman, I., Svergun, D. I. and Sussman, J. L.** (2009). The quaternary structure of amalgam, a *Drosophila* neuronal adhesion protein, explains its dual adhesion properties. *Biophysical Journal* **97**, 2316–2326.
- Zhang, L. and Ward, R. E.** (2009). uninflatable encodes a novel ectodermal apical surface protein required for tracheal inflation in *Drosophila*. *Developmental Biology* **336**, 201–212.

Figures

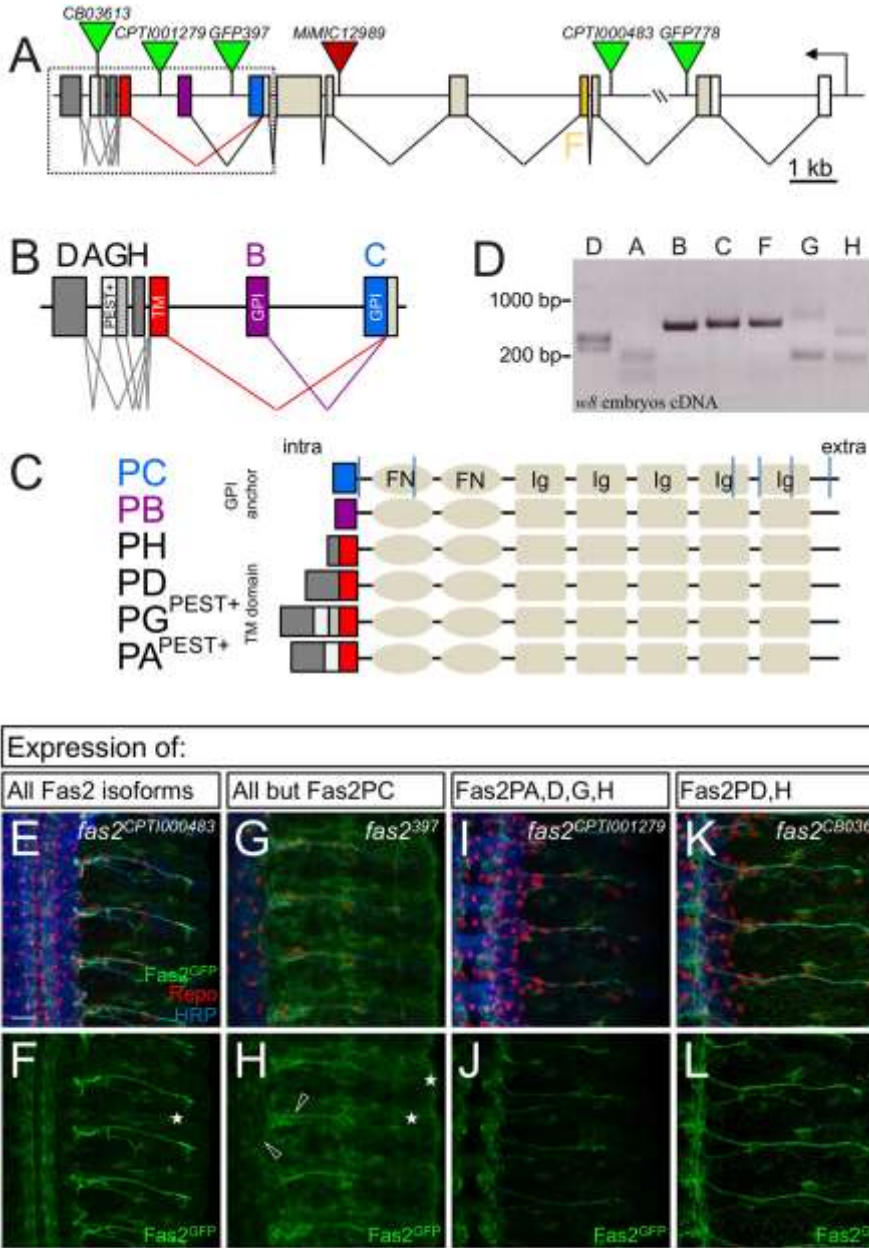
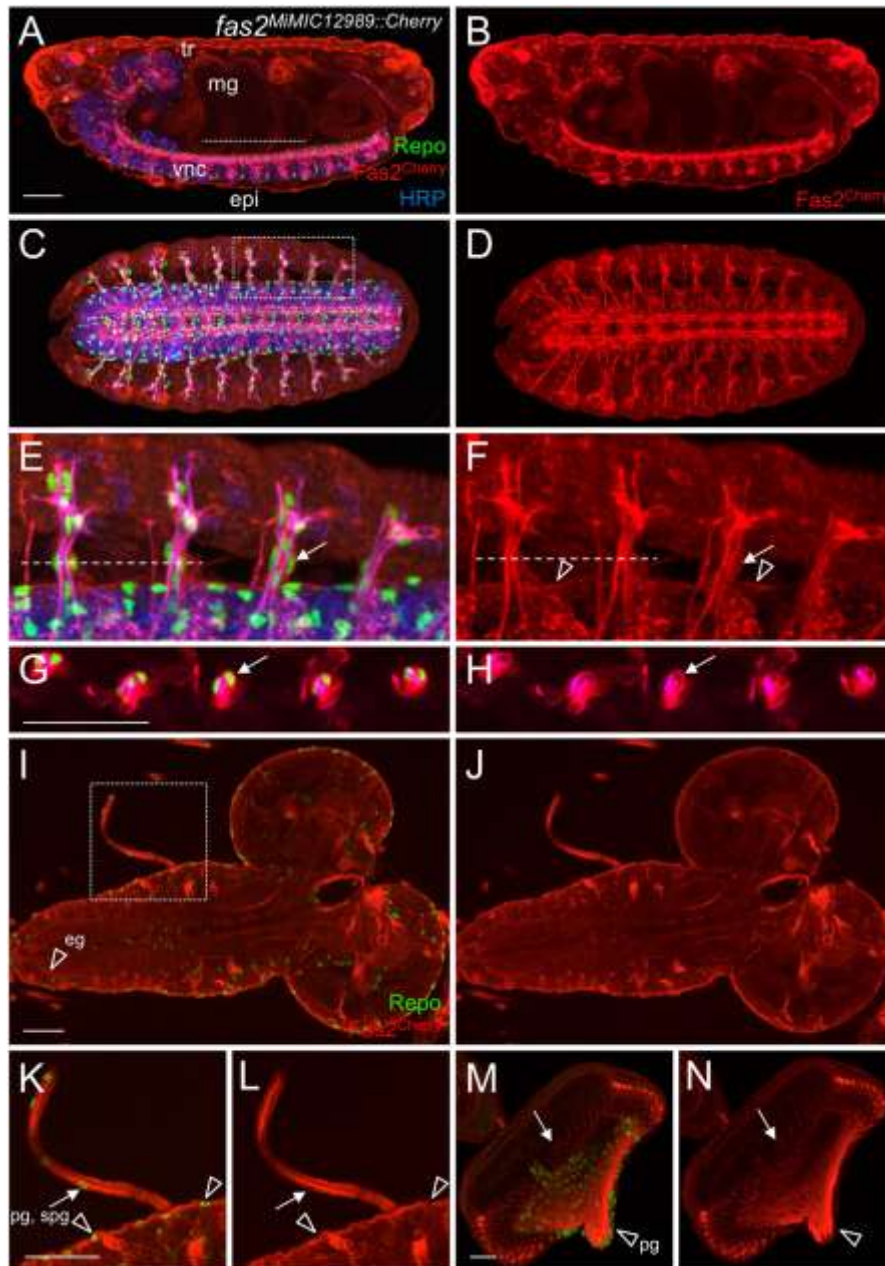


Figure 1 Different isoforms of the *fasciclin 2* locus

A) Schematic view of the *fas2* locus organization. Transcription is from right to left. Only one promoter region is present. The positions of several exon trap or MiMIC transposon insertions that have been utilized to determine the expression pattern of

the different Fas2 isoforms are depicted. The exons are color coded corresponding to the seven Fas2 isoforms. B) Higher magnification of the 3' end of the *fas2* gene. The organization of the different isoforms is indicated. Isoforms PB and PC are linked by a GPI-anchor. All other isoforms share a common transmembrane domain and variable cytoplasmic domains. C) Organization of the principle Fas2 proteins. Ig: Ig-domain, FN: fibronectin type III domain. The color coding is as shown in (A,B). The vertical blue lines in protein structure indicate the position of the introns. D) Expression of all predicted isoforms was tested by RT-PCR using exon specific primer combinations. cDNA Fragments of the expected length were detected that differed from amplification products using genomic DNA. RARD (genomic: 1,500 bp, cDNA: 300/390 bp); RA (genomic: 850 bp, cDNA: 240 bp); RB (genomic 1,500 bp, cDNA: 560bp); RC (genomic 680 bp, cDNA: 580 bp); RF (genomic: 11,154 bp, cDNA: 600 bp); RG (genomic: 750 bp, cDNA 240 bp); RH (genomic: 500 bp, cDNA 220 bp). Expression of the isoforms PB, PC and PF can be detected most robustly. E-L) Staining of stage 15 embryos ( $n > 10$  per genotype) carrying different exon trap elements that allow detection of the GFP-tagged Fas2 isoforms as indicated. Embryos are stained for expression of GFP to detect expression of the endogenously tagged Fas2<sup>GFP</sup> fusion proteins (green), Repo to label glial nuclei (red) and HRP (blue) to show all neuronal membranes. Stars in (F,H) denote epidermal Fas2 expression, arrowheads indicate glial staining. Scale bar is 20 $\mu$ m.



**Figure 2 Expression of all Fas2 isoforms as detected by *MiMIC12989-Cherry***

Expression of a Fas2::mCherry fusion generated by inserting a cherry exon into the *MiMIC12989* element, (n>10 animals were analyzed). A-H) Expression of Fas2::mCherry in stage 16 embryos. A,B) Lateral view. Anterior is to the left, dorsal is up. HRP staining (blue) detects all neuronal membranes, Repo (green) marks all glial

nuclei. During embryonic development a robust Cherry expression can be detected outside of the ventral nerve cord (VNC) in the epidermis (epi), tracheal cells (tr) and the midgut (mg). Scale bar is 50  $\mu$ m. C,D) Ventral view. The boxed area is shown in higher magnification in (E,F). E,F) Fas2::mCherry is expressed by glial cells. This can be seen at the segmental nerves (arrow) and the glial blood-brain barrier (arrowheads). The dashed line indicates the position of the orthogonal sections shown in (G,H, scale bar is 50  $\mu$ m). I-L) Expression of Fas2::mCherry in the third instar larval brain. I,J) Broad expression is found in the larval brain. Note that the characteristic expression pattern of Fas2 in a subset of axonal fascicles is not visible in the focal plane shown. Instead, expression in the ensheathing glia which encase the entire neuropil is visible (arrowhead, eg). The boxed area is shown in higher magnification in (K,L). K,L) Expression of Fas2::mCherry in glial cells. Expression can be seen in glial cells of the blood-brain barrier (arrowheads). It cannot be resolved whether perineurial (pg) and subperineurial glial cells (spg) express Fas2::mCherry. M,N) Expression in the eye-imaginal disc. Neuronal and glial expression can be detected. Glial expression is found in the perineurial glia (pg, arrowhead) and the wrapping glia (arrow). (I-N) Scale bars are 20  $\mu$ m.

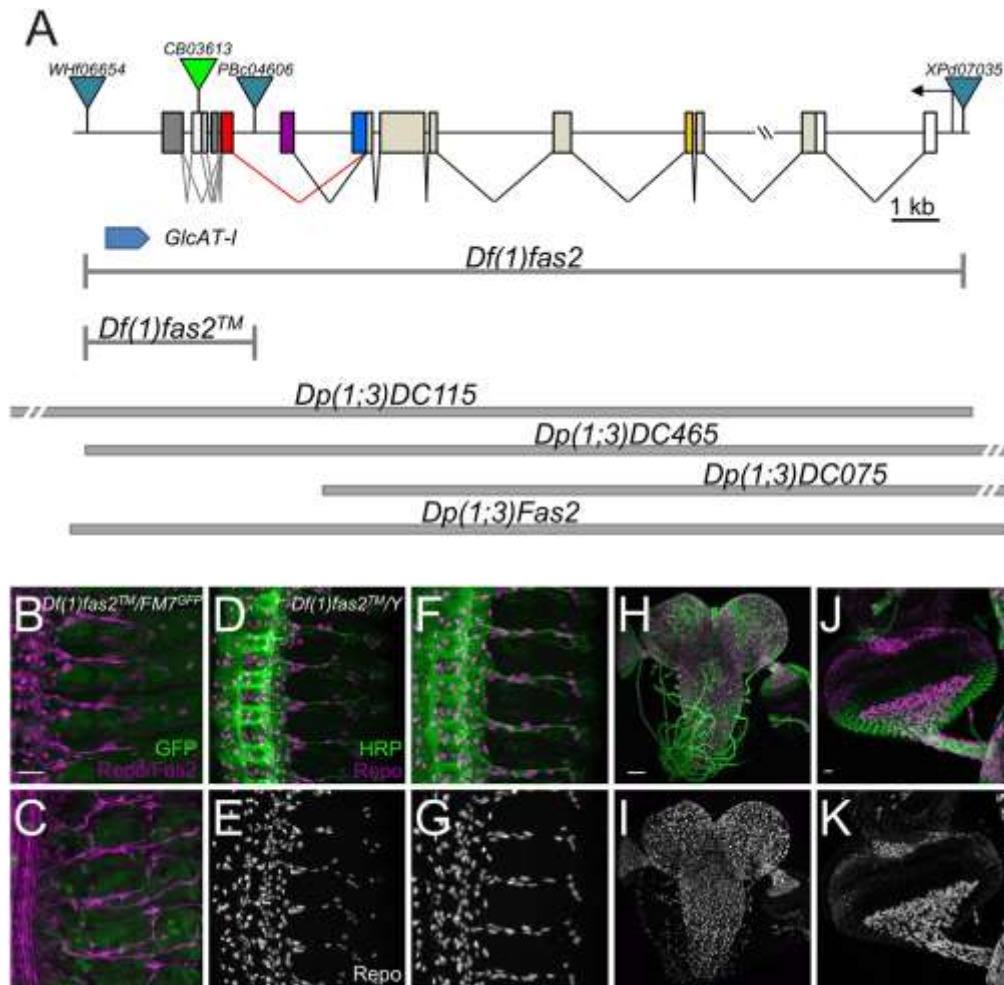


**Figure 3 Generation of *fasciclin 2* null alleles and rescue experiments**

A) Schematic view of the *fas2* locus organization as described in Figure 1. The triangles indicate the insertion of the different transposons used during the mutant analysis. The turquoise colored triangles represent FRT bearing transposons used to generate deficiencies *Df(1)fas2* and *Df(1)fas2<sup>TM</sup>* as indicated. All Bac-based duplications are shown. B-K) Immunohistochemically analysis of embryos (B-G) and larval brain with eye-imaginal discs (H-K), scale bars are 20  $\mu$ m,  $n > 10$  animals analyzed. Anti-Fas2 (mAb 1D4), and anti-Repo are shown in magenta, GFP (B,C), and anti-HRP (D-K) staining is in green. B,C) In heterozygous stage 14 (B), or stage



16 (C) embryos of the genotype *Df(1)fas2<sup>TM</sup>/FM7<sup>twiGFP</sup>* Fas2 expression can be detected. Weak GFP expression due to the balancer is detected. D-F) In contrast, in *Df(1)fas2<sup>TM</sup>* mutant embryos (D: stage 14; F: stage 16), no expression of the anti-1D4 antigen is detected. Loss of membrane bound Fas2 proteins does not lead to abnormal glial or neuronal phenotypes. H,I) Similarly, in *Df(1)fas2<sup>TM</sup>* mutant larval brains, or (J,K) eye-imaginal discs no abnormal neural phenotypes can be detected. Note that no Fas2 staining can be detected since the cytoplasmic Fas2 domain is deleted and thus the mAb 1D4 antigen is absent.

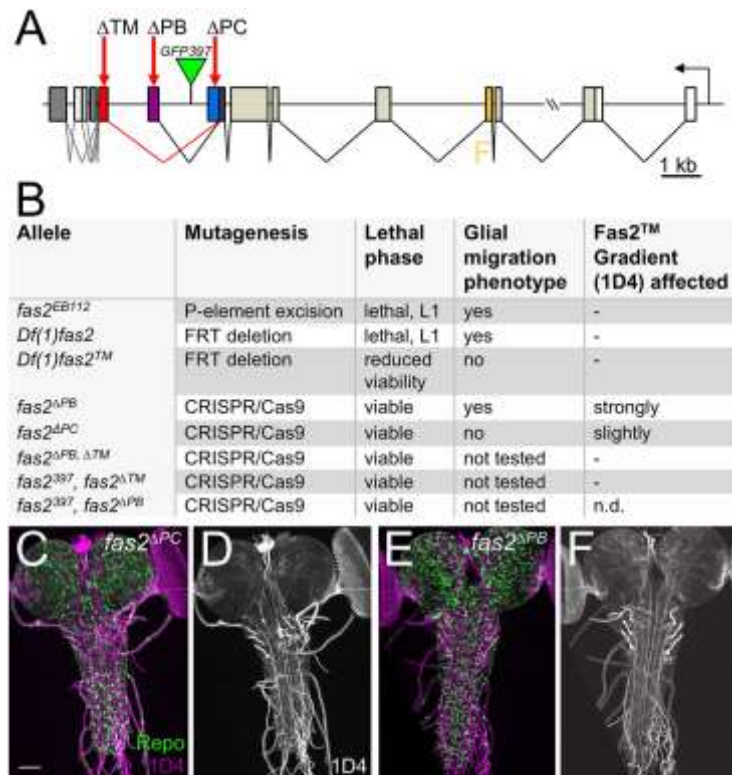


**Figure 4 Generation of isoform specific *fasciclin 2* mutants**

A) Schematic view of the *fas2* locus with the position of all CRISPR induced mutations indicated by red arrows. Some of the mutants were generated in the background of the exon trap line *fas2*<sup>GFP397</sup> which allows the detection of all Fas2 isoforms except Fas2<sup>PC</sup>. B) Table summarizing all *fas2* alleles generated in this study. The results of the phenotypic analysis are summarized, n>10 animals were analyzed. C,D) Third instar larval brain of a homozygous *fas2*<sup>PC</sup> mutant stained for Fas2<sup>TM</sup> (anti-1D4, magenta) and Repo (green). No abnormal neural phenotype can be detected. E,F) Third instar larval brain of a homozygous *fas2*<sup>PB</sup> mutant stained for Fas2<sup>TM</sup> (anti-1D4, magenta) and Repo (green). No abnormal neural phenotype can be detected. The scale bar is 20 μm.

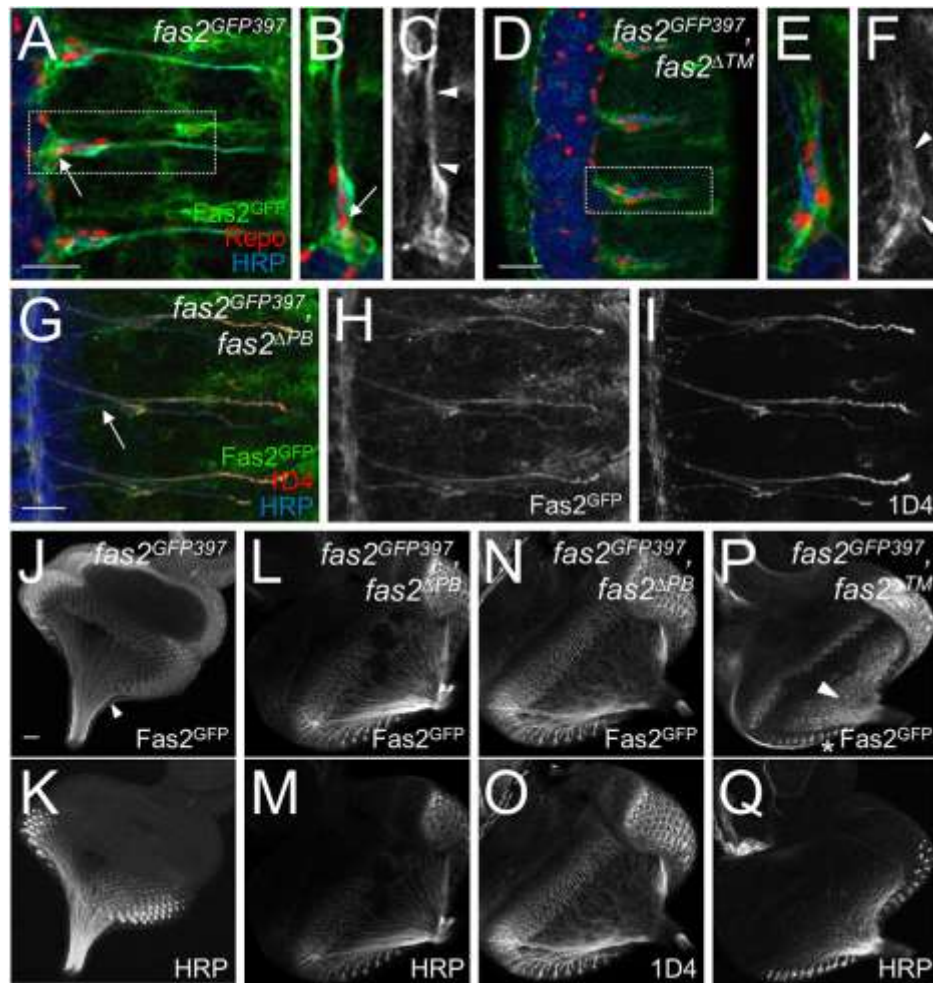


**Figure 5 Fas2<sup>PB</sup> is expressed by glial cells**

A) Homozygous *fas2<sup>GFP397</sup>* embryo stained for Fas2::GFP expression (green), Repo (red) and HRP (blue). The dashed area is shown in higher magnification in (B,C). Note that little GFP expression is found on glial cell bodies (arrow). Most GFP-expression is found along segmental nerves (arrowheads). D) Homozygous *fas2<sup>GFP397</sup>, fas2<sup>ΔTM</sup>* mutant embryo. The dashed area is shown in higher magnification in (E,F). Note, the broader expression of GFP which is not confined to segmental nerves, but is found in the entire glial cell body. G-I) Homozygous *fas2<sup>GFP397</sup>, fas2<sup>ΔPB</sup>* mutant embryo. Neuronal expression of Fas2 is still visible. Note, the even

expression of Fas2 along the motor axon. Glial expression is absent. J,K) Third instar larval *fas2<sup>GFP397</sup>* eye-imaginal disc stained for expression of GFP (J) and HRP (K). L-O) Third instar larval *fas2<sup>GFP397</sup>*, *fas2<sup>ΔPB</sup>* mutant eye-imaginal discs. L,N) GFP expression is found along photoreceptor axons. M) HRP expression and (O) 1D4 expression label photoreceptor neurons. P,Q) Third instar larval *fas2<sup>GFP397</sup>*, *fas2<sup>ΔTM</sup>* mutant eye-imaginal disc. P) Note the broad GFP expression in glial cells (arrowhead). Asterisk denotes expression in photoreceptor neurons. Q) Neuronal HRP expression is normal. The scale bar is 20μm, n>10 embryos (A-I) or eye imaginal discs (J-Q) were analyzed for each genotype.

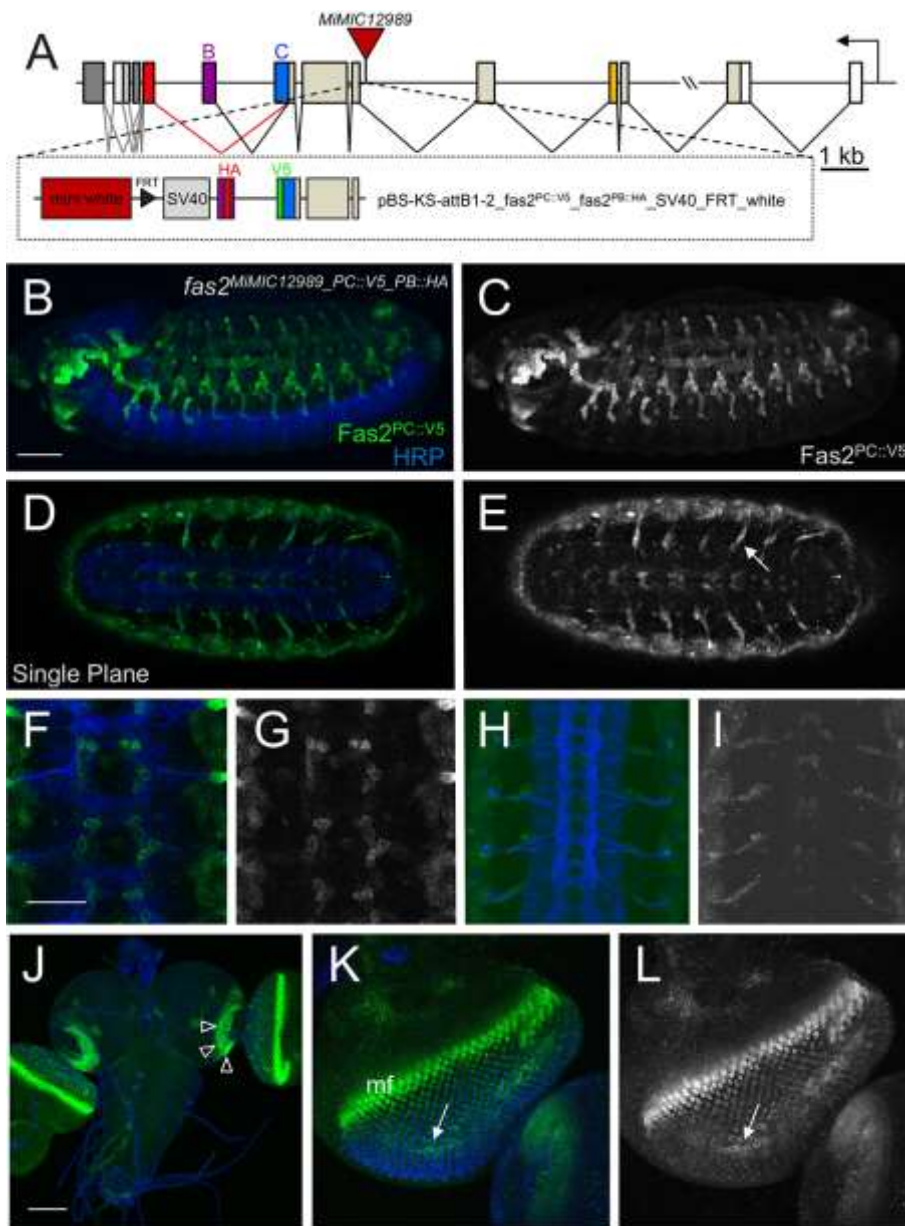


**Figure 6 Fas2<sup>PC</sup> is expressed in non-neuronal cells**

A) Schematic view of the *fas2* locus, showing the construct used to follow Fas2<sup>PC</sup> expression was inserted into the *Mi{MIC}Fas2<sup>Mi12989</sup>* piggyback insertion. B-E) Stage 15 embryos expressing V5-tagged Fas2<sup>PC</sup>. Anterior is to the left, (B,C) lateral view, dorsal up, (D,E) ventral view. Scale bar is 50  $\mu$ m. Note the strong expression of Fas2<sup>PC</sup> in cells of the tracheal system and some neurons. F,G) High magnification of

a stage 14 embryo showing Fas2<sup>PC</sup> expression in the CNS. Scale bar is 20  $\mu$ m. H,I) High magnification of a stage 16 embryo showing Fas2<sup>PC</sup> expression in the CNS. J) Expression of Fas2<sup>PC</sup> in a third instar larval brain and (K,L) the attached eye-antennal discs. Note the strong expression in a crescent of cells in the larval brain lobes (arrowheads), the morphogenetic furrow (mf) and expression in glial cells of the eye-imaginal disc (arrowhead in L). Scale bar is 50  $\mu$ m, n>10 embryos (A-I) or eye imaginal discs (J-Q) were analyzed for each genotype.

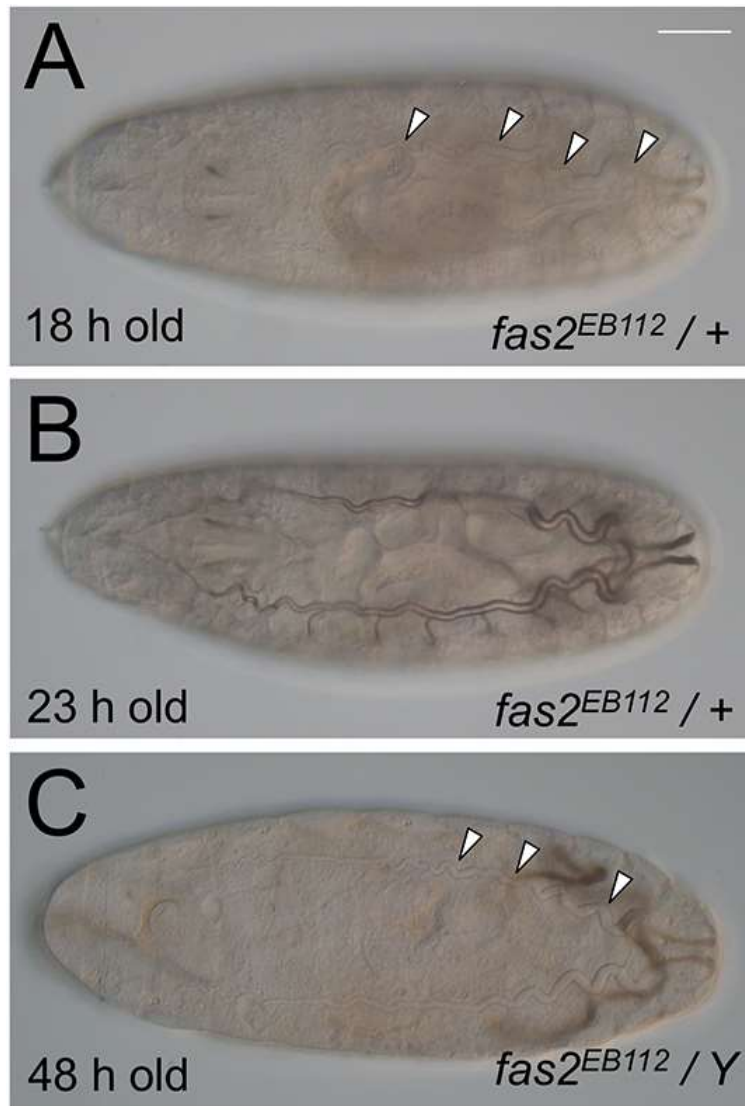


**Figure 7 *fas2* mutants have a defective tracheal system**

A) 18 h old heterozygous *fas2<sup>EB112</sup>* embryo. The tracheal system including the dorsal trunk (arrowheads) is formed but not yet inflated. B) 23 h old heterozygous *fas2<sup>EB112</sup>* embryo, shortly before hatching. The tracheal system is now filled with air. C) 48 h old hemizygous *fas2<sup>EB112</sup>* mutant embryo. The tracheal system is still not filled with air. Scale bar is 50  $\mu$ m,  $n > 10$  embryos were analyzed for each genotype.

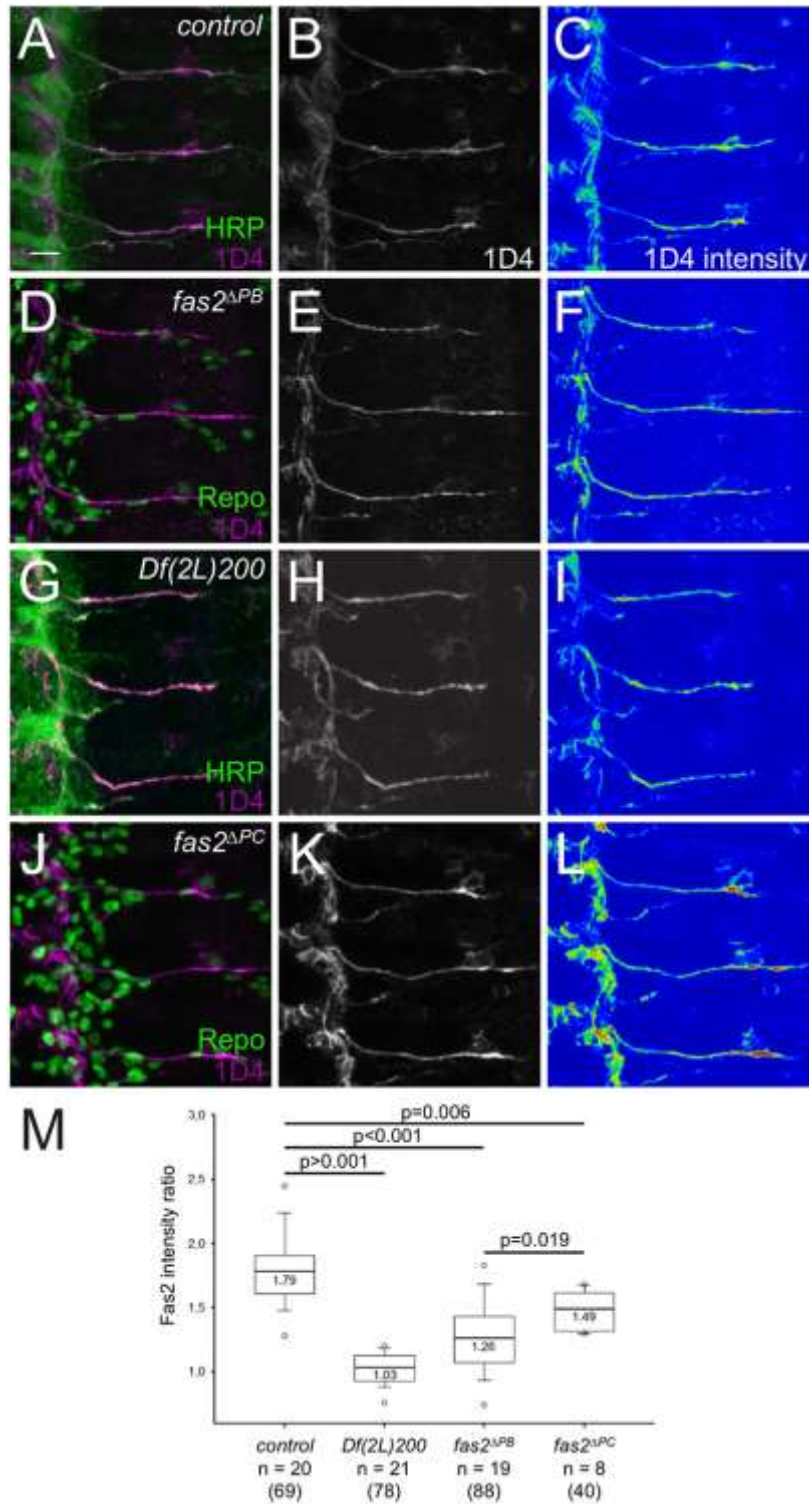


**Figure 8 Graded expression of neuronal Fas2™ isoform is caused by glial Fas2 expression**



Expression of the Fas2<sup>TM</sup> epitope (anti 1D4 staining) in stage 14 embryos (magenta). Neuronal membranes are in green (A,G) or glial cells are in green (D,J) False color images represent the expression strength of Fas2 along the motor axons (C,F,I,L). A-C) In wild type embryos, Fas2<sup>TM</sup> is expressed in a graded fashion along the axon, with a stronger expression towards the growth cone. For quantification see (M). D-F) This gradient is lost in homozygous *fas2<sup>ΔPB</sup>* mutant embryos. G-I) Likewise no graded Fas2<sup>TM</sup> expression can be detected in a *gcm*, *gcm2* mutant background. J-L) The graded distribution of Fas2<sup>TM</sup> is only slightly affected by removing the expression of Fas2<sup>PC</sup>. M) Statistics comparing the Fas2 intensity ratio on motor neurons at CNS/PNS boundary compared expression in the growth cone area, performing a Mann-Whitney Rank Sum test. Box-whisker plot represents the median (bold line), 25% and 75% quartiles (box), and 5% and 95% extreme values (circles). n: Number of embryos tested per genotype, the number given in brackets represents the number of analyzed hemisegments. Scale bar is 20μm. 8-20 embryos with 40-88 segments were analyzed as indicated.

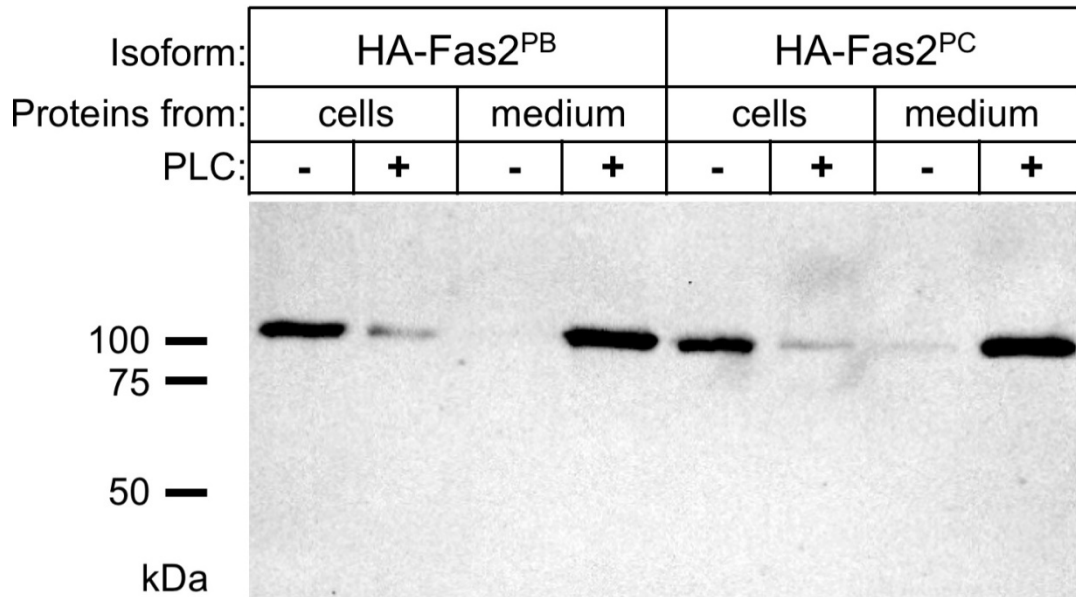


**Figure S1 Fas2<sup>PB</sup> and Fas2<sup>PC</sup> are GPI linked proteins**

Western blot analysis of S2 cells transfected with act5C-Gal4 together with either *UAS-HA-fas2<sup>PB</sup>* or *UAS-HA-fas2<sup>PC</sup>*. Cells were treated for 1 hour as indicated. Pellet and supernatant were analyzed separately. Both proteins are efficiently released to the supernatant (medium) by PiPLC treatment.

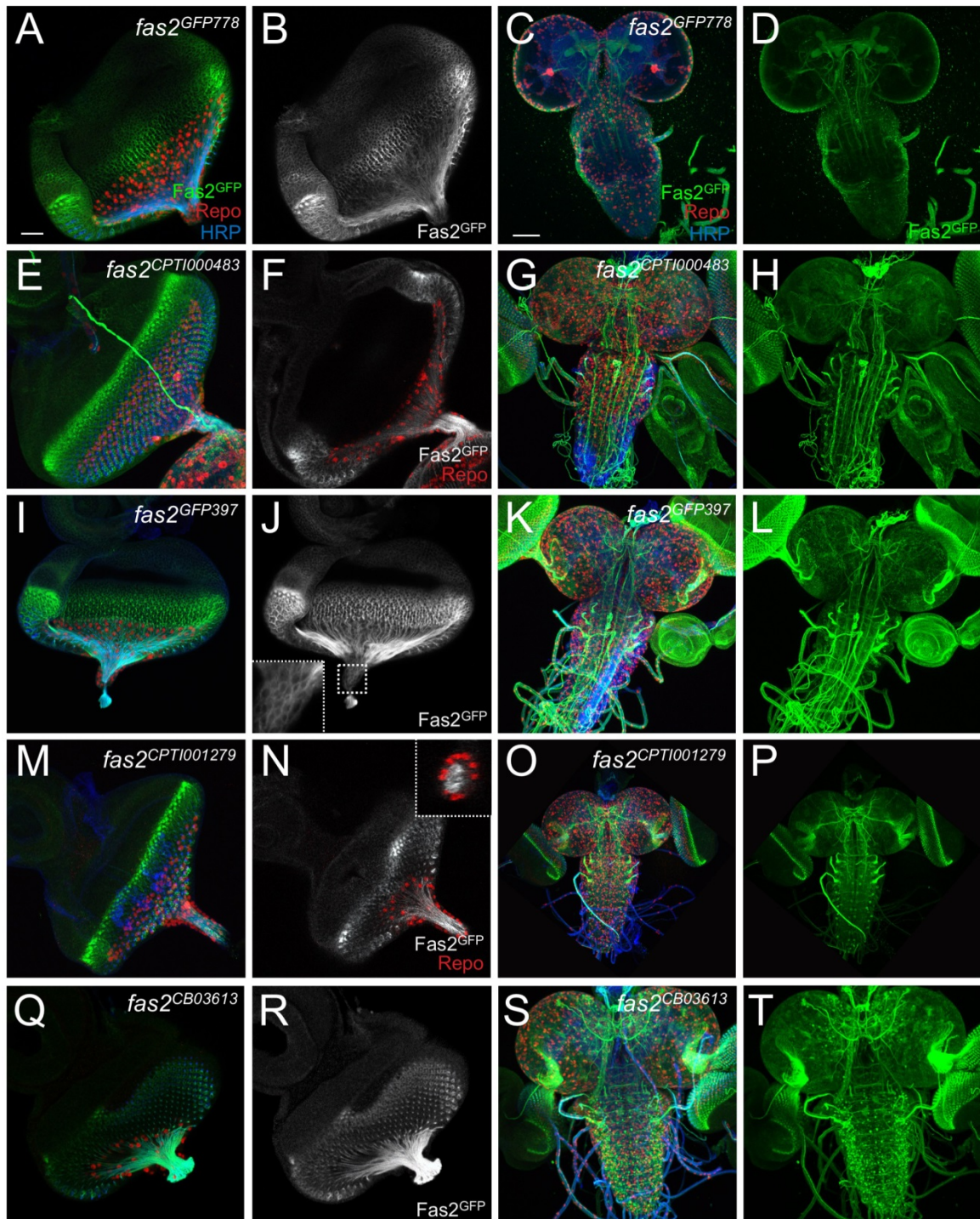


**Figure S2 GFP expression associated with different *fas2* gene traps**

Larval expression pattern of the different gene trap insertion lines used in this study. Eye-imaginal discs are shown on the left, larval third instar brains are shown on the right. Specimens are stained for GFP expression (green), Repo expression (red) and

HRP expression (blue). A-D) *fas2*<sup>GFP778</sup>, E-H) *fas2*<sup>CPT1000483</sup>, I-L) *fas2*<sup>GFP397</sup>, M-P) *fas2*<sup>CPT1001279</sup>, Q-T) *fas2*<sup>CB03613</sup>. The inset in (J) shows the optic stalk to visualize the glial expression domain. The inset in (N) shows a cross section through the optic stalk to visualize the neuronal expression domain. Scale bar for eye imaginal discs 20  $\mu\text{m}$ , scale bar for larval brain 50  $\mu\text{m}$ . n>10 animals per genotype were analyzed.

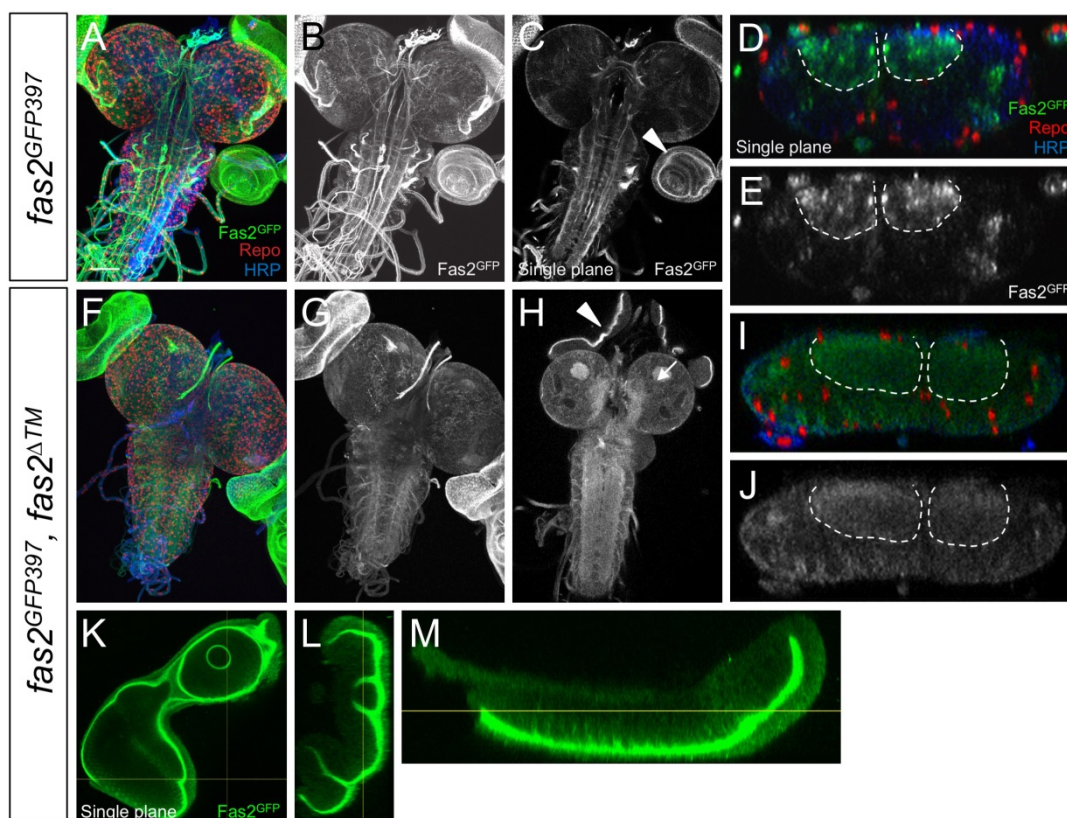


**Figure S3 Expression of  $fas2^{PB}$  changes in dependence of  $fas2^{TM}$**

A-M) Expression of the  $fas2^{GFP397}$  gene trap element. GFP expression is in green, Repo staining is shown in red, and HRP expression is shown in blue. Scale bar is 50  $\mu$ m. A-C) Third instar larval brain. Note the strong neuronal expression in the eye-imaginal discs. C) In a single confocal plane enhanced GFP expression is detected at the apical domain of imaginal disc cells (arrowhead). D,E) Note the strong neuronal expression of the  $Fas2^{TM}$  isoforms. Some GFP expression is detected throughout the neuropil. The dashed line indicates the neuropil boundary. F-H) Third instar larval brains of mutant  $fas2^{GFP397}, fas2^{TM}$  animals. The clear expression of Fas2 in CNS fascicles is lost. In addition, diffuse expression in the mushroom bodies is detected (arrow in H). I,J) The expression along axonal membranes in the neuropil is lost. Instead diffuse expression throughout the entire nervous system can be

detected. The dashed line indicates the neuropil boundary. K-M) Single confocal plane of an eye-imaginal disc of a mutant *fas2*<sup>GFP397</sup>, *fas2*<sup>TM</sup> animal. Note the strong expression of Fas2 in the interior lumen of the imaginal disc. n>10 animals per genotype were analyzed.

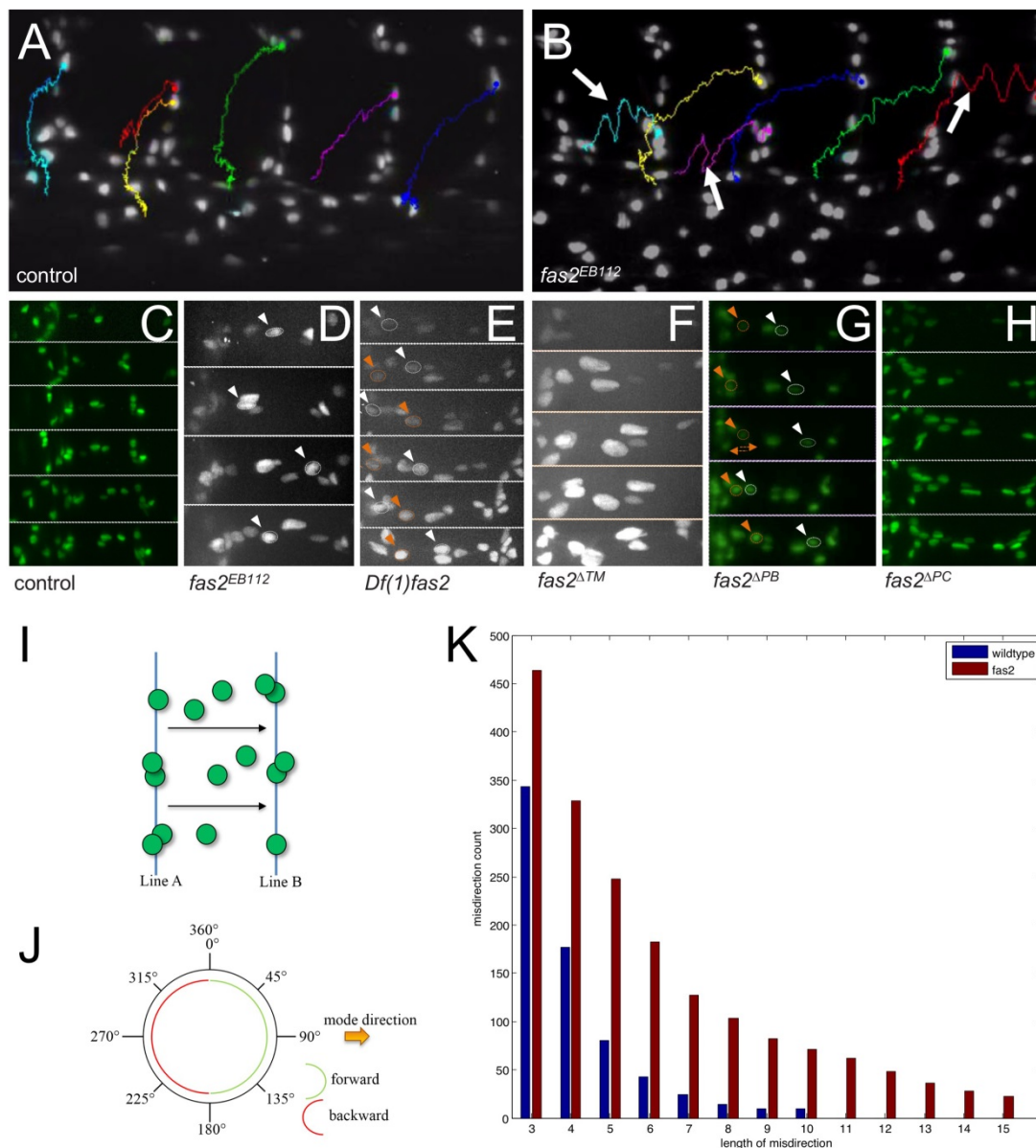


### Figure S4 *Fas2<sup>PB</sup>* is required for correct positioning of glial nuclei during embryonic development

The Figure shows stills of movies of embryonic development of the genotypes as indicated. Glial nuclei were imaged using a *repo-stinger::GFP* fusion. A) In wild type animals, peripheral glial cells born in the CNS/PNS transition zone move outwards to peripheral positions. The colored lines follow the movement of an individual glial cell. Note the straight migration towards the periphery. B) *fas2<sup>EB112</sup>* mutant animal. Note the backwards movement of glial nuclei in several segments (arrows). C-H) Consecutive frames of a movie showing the migration of the peripheral glial cells. C) Control embryo. D) *fas2<sup>EB112</sup>* mutant animal. E) *Df(1)fas2* mutant animal. F) *Df(1)fas2<sup>f</sup>* mutant

animal. G)  $fas2^{a}$  and (H)  $fas2^{a}$  mutant animal. In  $fas2$  mutants affecting the expression of  $Fas2^{PB}$  ( $fas2^{EB112}$ ,  $Df(1)fas2$ ,  $fas2^{a}$ ) glial nuclei often move backwards as indicated (white and orange arrowheads). For detailed imaging see supplementary movies 1-6. I) Schematic view of glial movement from line A to line B. All movements from A to B in angles as indicated in (J) where rated as forward, movements from line B to line A where rated as backward. K) Quantification of length of backwards movement. The x-axis gives the length of misdirection in frames of movies imaged with 1 frame per minute. The y-axis indicates number of sequences observed in the different movies. 30-40 individual glial cell nuclei were tracked per movie. *control*: n= movies from 4 embryos, " $go^{EB112}$ ": n=movies from 7 embryos.



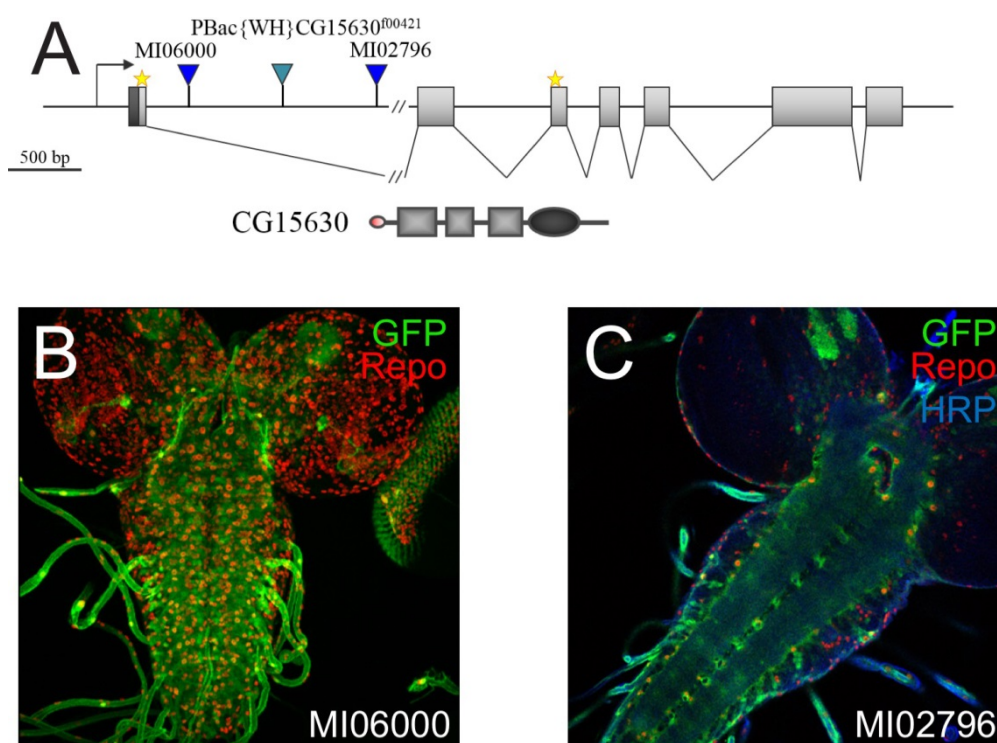


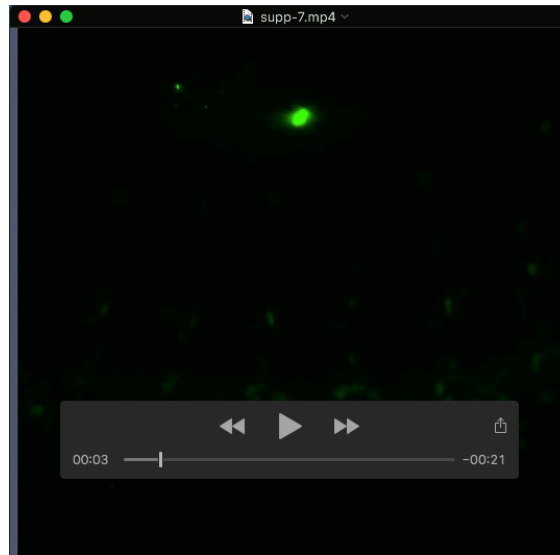
**Figure S5 Expression of *CG15630* in the larval nervous system**

A) Schematic view of the *CG15630* gene locus. The insertion of two MiMIC transposon insertions is indicated. Transcription is from left to right. B) GFP expression directed by the MiMIC insertion MI06000. Green: GFP expression, red show expression of the Repo protein which labels glial cell nuclei. C) GFP expression directed by the MiMIC insertion MI02796. Staining is as in (B).  $n > 6$  brains were analyzed per genotype.



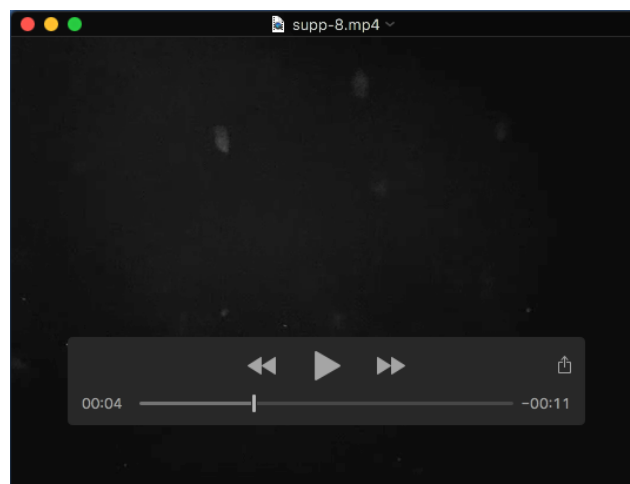
**Figure S6 Details of the different isoform specific *fas2* mutations**

The figure shows the mutations generated using CRISPR/Cas9. The PAM and the target sequence are indicated by shading. The triangle indicates the predicted cleavage sites. The underlined triplets encode amino acids that can be used for GPI-anchor addition.



### Movie 1

Stage 14 control embryo carrying a *repo-stGFP* element to label glial nuclei.



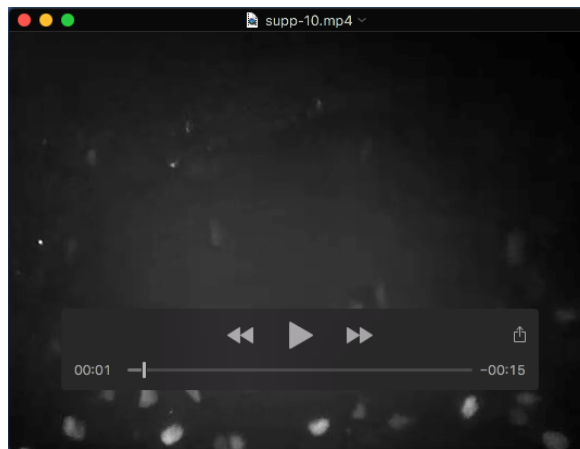
### Movie 2

Stage 14 *fas2*<sup>EB112</sup> mutant embryo carrying a *repo-stGFP* element to label glial nuclei.



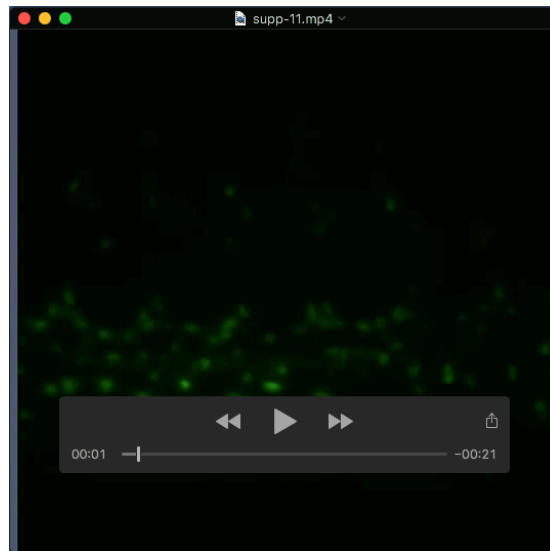
### Movie 3

Stage 14 *Df(Df(i g" 3* mutant embryo carrying a *repo-stGFP* element to label glial nuclei.



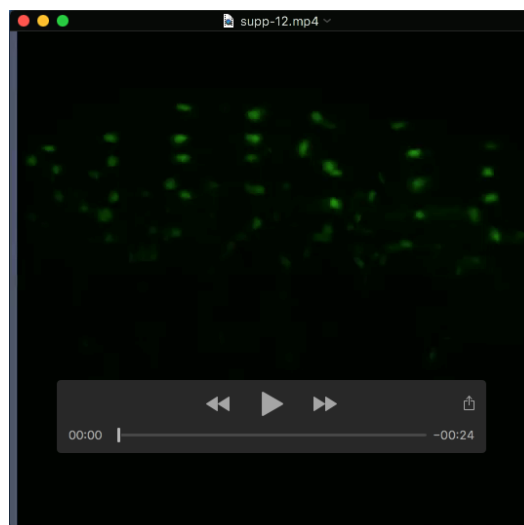
### Movie 4

Stage 14 *fas2<sup>aa</sup>* mutant embryo carrying a *repo-stGFP* element to label glial nuclei.



### Movie 5

Stage 14 *fas2*<sup>''<sup>a</sup></sup> mutant embryo carrying a *repo-stGFP* element to label glial nuclei.



### Movie 6

Stage 14 *fas2*<sup>''<sup>a</sup></sup> mutant embryo carrying a *repo-stGFP* element to label glial nuclei.

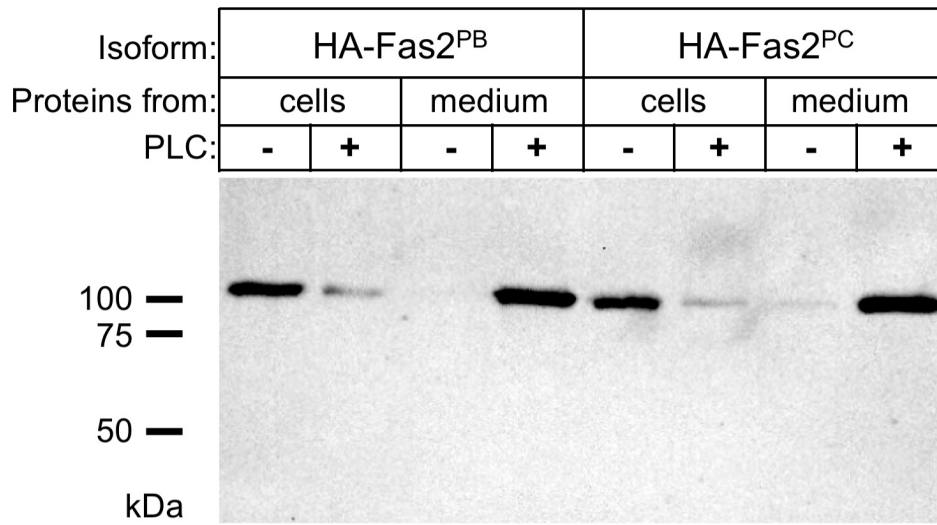


### Figure S1 Fas2<sup>PB</sup> and Fas2<sup>PC</sup> are GPI linked proteins

Western blot analysis of S2 cells transfected with act5C-Gal4 together with either *UAS-HA-Fas2<sup>PB</sup>* or *UAS-HA-Fas2<sup>PC</sup>*. Cells were treated for 1 hour as indicated. Pellet and supernatant were analyzed separately. Both proteins are efficiently released to the supernatant (medium) by PiPLC treatment.

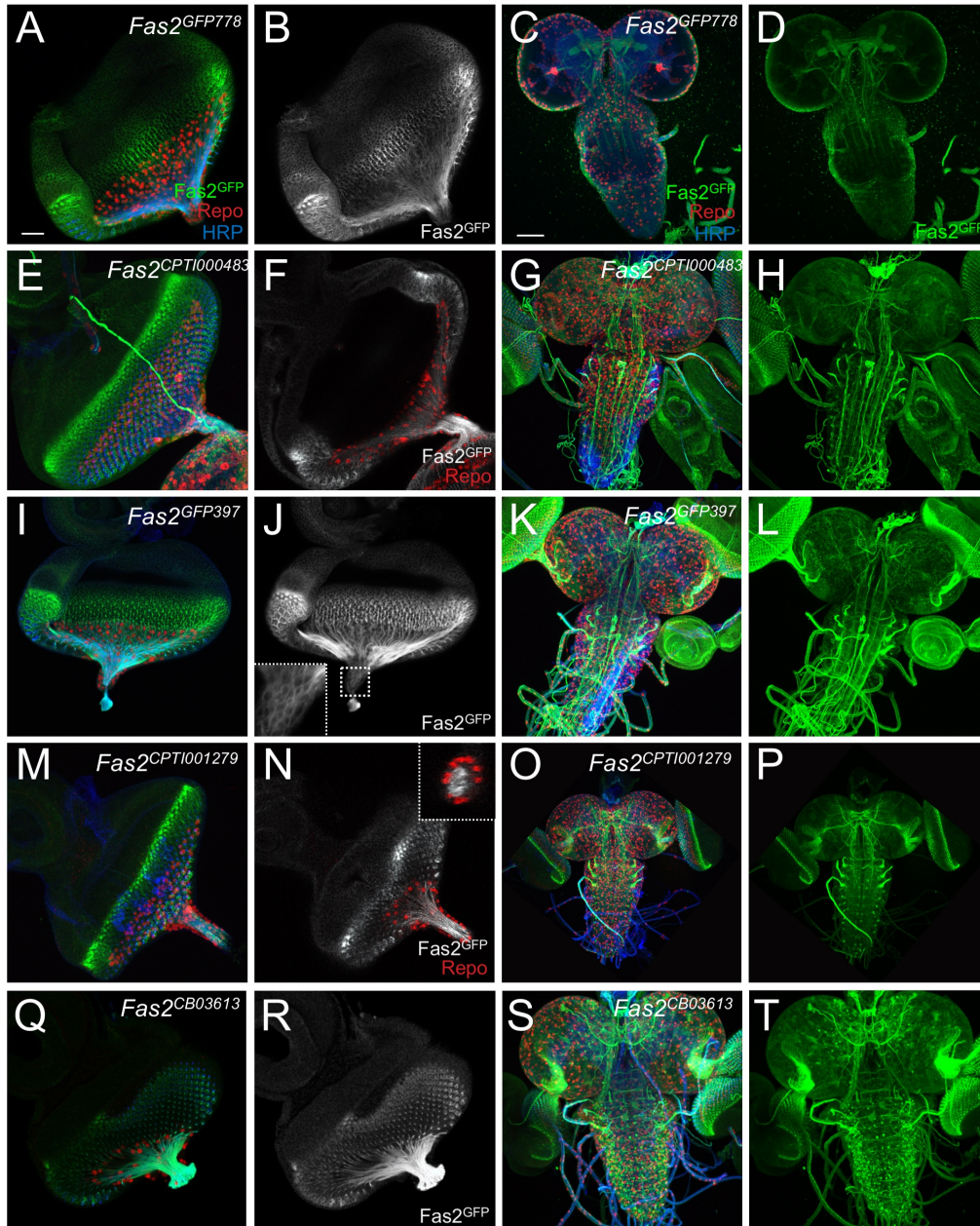


**Figure S2** GFP expression associated with different *Fas2* gene traps

Larval expression pattern of the different gene trap insertion lines used in this study. Eye-imaginal discs are shown on the left, larval third instar brains are shown on the right. Specimens are stained for GFP expression (green), Repo expression (red) and

HRP expression (blue). A-D) *Fas2*<sup>GFP778</sup>, E-H) *Fas2*<sup>CPT1000483</sup>, I-L) *Fas2*<sup>GFP397</sup>, M-P) *Fas2*<sup>CPT1001279</sup>, Q-T) *Fas2*<sup>CB03613</sup>. The inset in (J) shows the optic stalk to visualize the glial expression domain. The inset in (N) shows a cross section through the optic stalk to visualize the neuronal expression domain. Scale bar for eye imaginal discs 20  $\mu\text{m}$ , scale bar for larval brain 50  $\mu\text{m}$ . n>10 animals per genotype were analyzed.



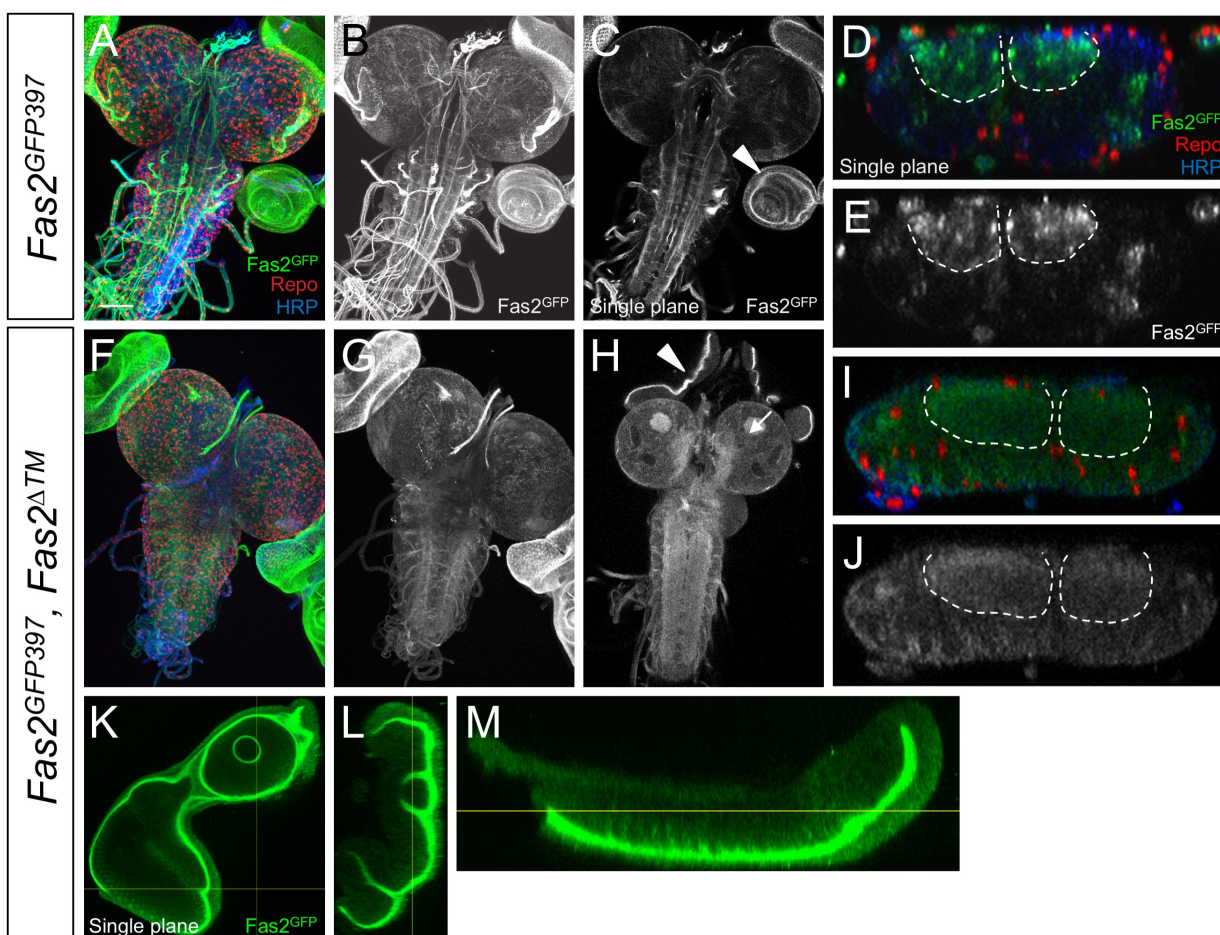


**Figure S3 Expression of *Fas2*<sup>PB</sup> changes in dependence of *Fas2*<sup>TM</sup>**

A-M) Expression of the *Fas2*<sup>GFP397</sup> gene trap element. GFP expression is in green, Repo staining is shown in red, and HRP expression is shown in blue. Scale bar is 50 μm. A-C) Third instar larval brain. Note the strong neuronal expression in the eye-imaginal discs. C) In a single confocal plane enhanced GFP expression is detected at the apical domain of imaginal disc cells (arrowhead). D,E) Note the strong neuronal expression of the *Fas2*<sup>TM</sup> isoforms. Some GFP expression is detected throughout the neuropil. The dashed line indicates the neuropil boundary. F-H) Third instar larval brains of mutant *Fas2*<sup>GFP397</sup>, *Fas2*<sup>ΔTM</sup> animals. The clear expression of Fas2 in CNS fascicles is lost. In addition, diffuse expression in the mushroom bodies is detected (arrow in H). I,J) The expression along axonal membranes in the neuropil is lost. Instead diffuse expression throughout the entire nervous system can be

detected. The dashed line indicates the neuropil boundary. K-M) Single confocal plane of an eye-imaginal disc of a mutant *Fas2*<sup>GFP397</sup>, *Fas2*<sup>TM</sup> animal. Note the strong expression of Fas2 in the interior lumen of the imaginal disc. n>10 animals per genotype were analyzed.

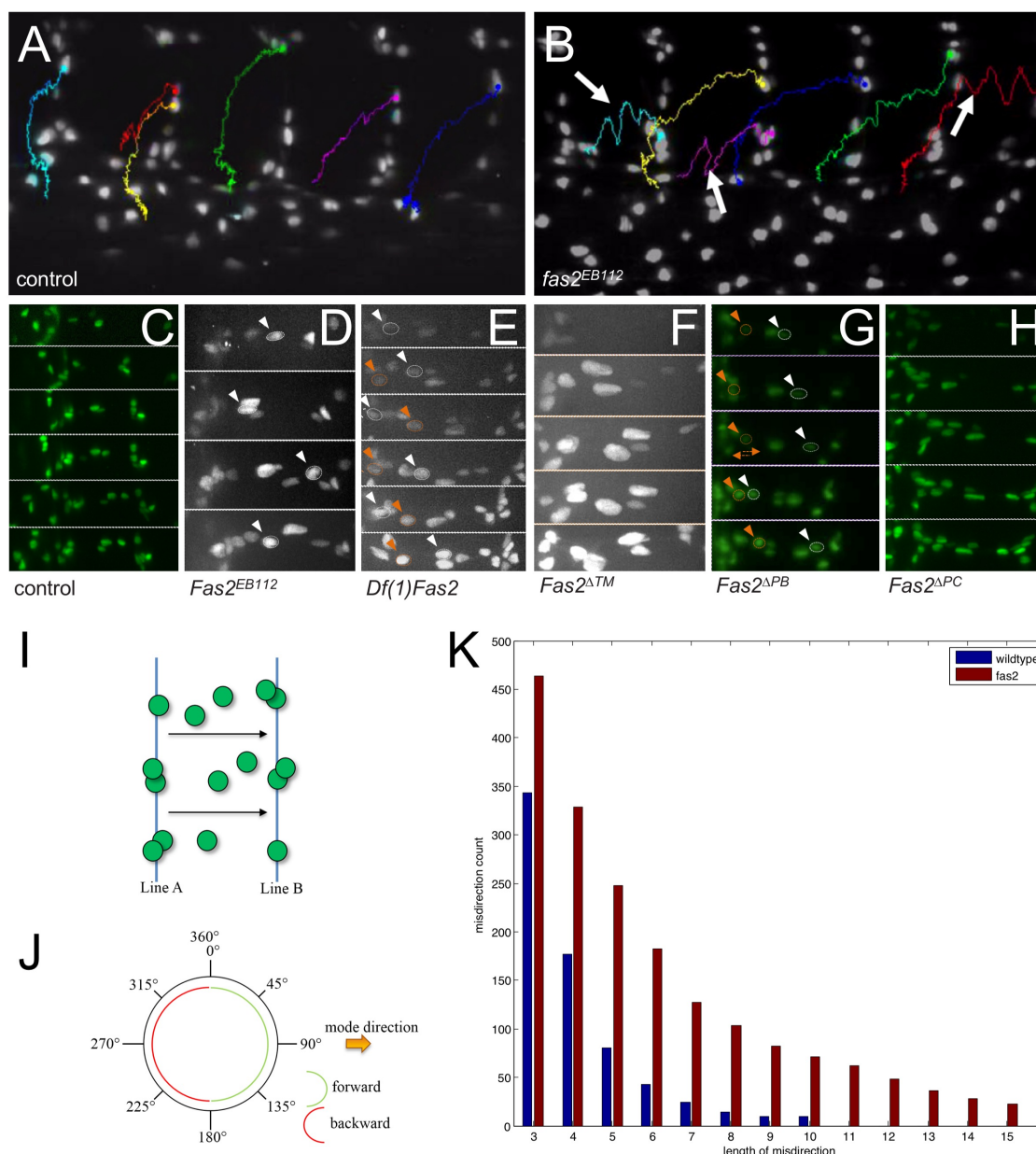


### Figure S4 *Fas2<sup>PB</sup>* is required for correct positioning of glial nuclei during embryonic development

The Figure shows stills of movies of embryonic development of the genotypes as indicated. Glial nuclei were imaged using a *repo-stinger::GFP* fusion. A) In wild type animals, peripheral glial cells born in the CNS/PNS transition zone move outwards to peripheral positions. The colored lines follow the movement of an individual glial cell. Note the straight migration towards the periphery. B) *Fas2<sup>EB112</sup>* mutant animal. Note the backwards movement of glial nuclei in several segments (arrows). C-H) Consecutive frames of a movie showing the migration of the peripheral glial cells. C) Control embryo. D) *Fas2<sup>EB112</sup>* mutant animal. E) *Df(1)Fas2* mutant animal. F) *Df(1)Fas2<sup>f</sup>* mutant

animal. G)  $Fas2^{a/a}$  and (H)  $Fas2^{EB112/a}$  mutant animal. In  $Fas2$  mutants affecting the expression of  $Fas2^{PB}$  ( $Fas2^{EB112}$ ,  $Df(1)Fas2$ ,  $Fas2^{a/a}$ ) glial nuclei often move backwards as indicated (white and orange arrowheads). For detailed imaging see supplementary movies 1-6. I) Schematic view of glial movement from line A to line B. All movements from A to B in angles as indicated in (J) where rated as forward, movements from line B to line A where rated as backward. K) Quantification of length of backwards movement. The x-axis gives the length of misdirection in frames of movies imaged with 1 frame per minute. The y-axis indicates number of sequences observed in the different movies. 30-40 individual glial cell nuclei were tracked per movie. *control*: n= movies from 4 embryos, " $go^{EB112}$ ": n=movies from 7 embryos.

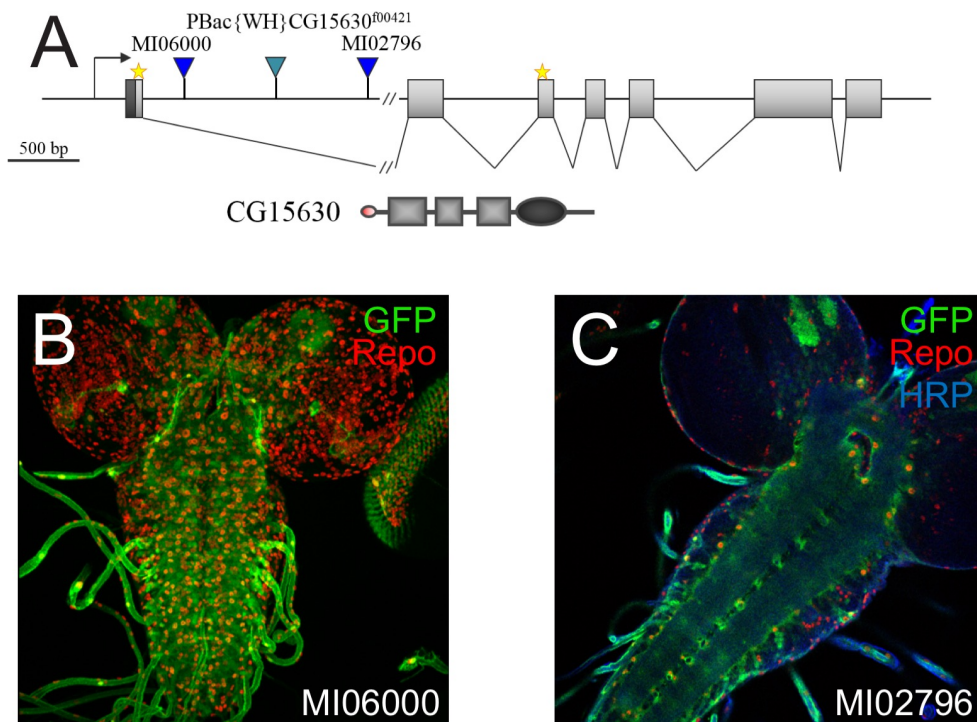


**Figure S5 Expression of *CG15630* in the larval nervous system**

A) Schematic view of the *CG15630* gene locus. The insertion of two MiMIC transposon insertions is indicated. Transcription is from left to right. B) GFP expression directed by the MiMIC insertion MI06000. Green: GFP expression, red show expression of the Repo protein which labels glial cell nuclei. C) GFP expression directed by the MiMIC insertion MI02796. Staining is as in (B).  $n > 6$  brains were analyzed per genotype.

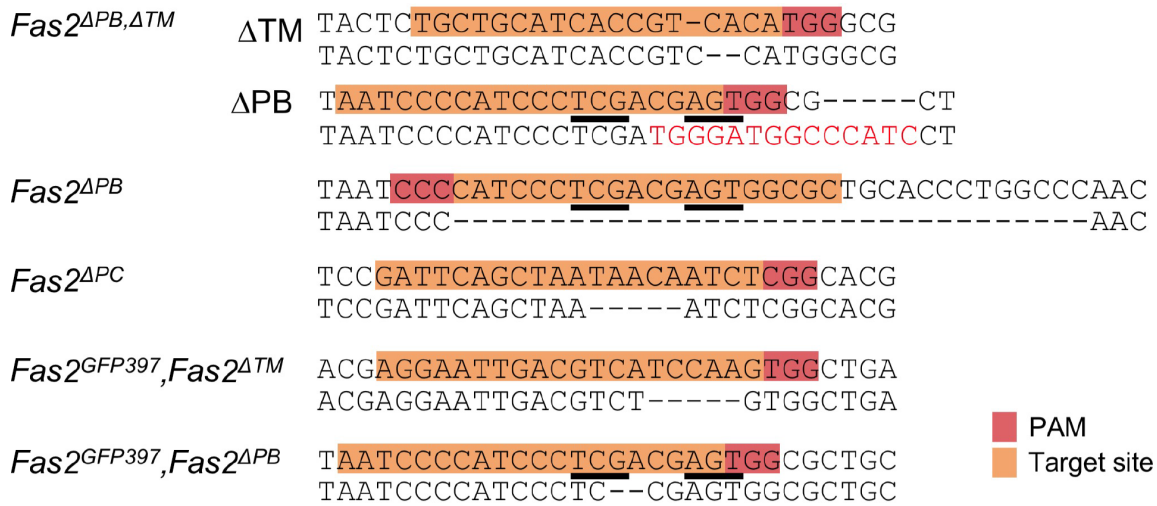
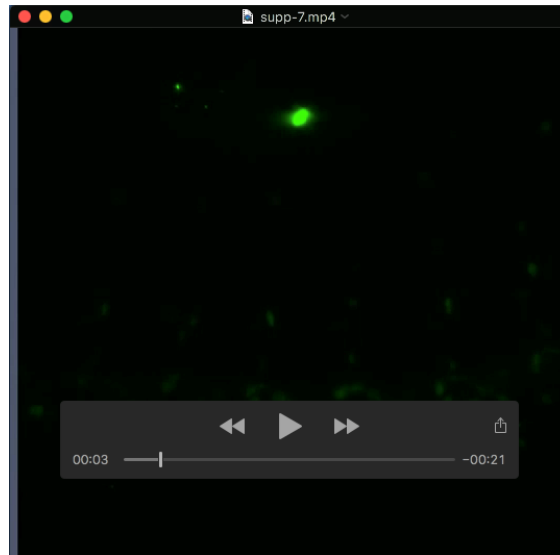


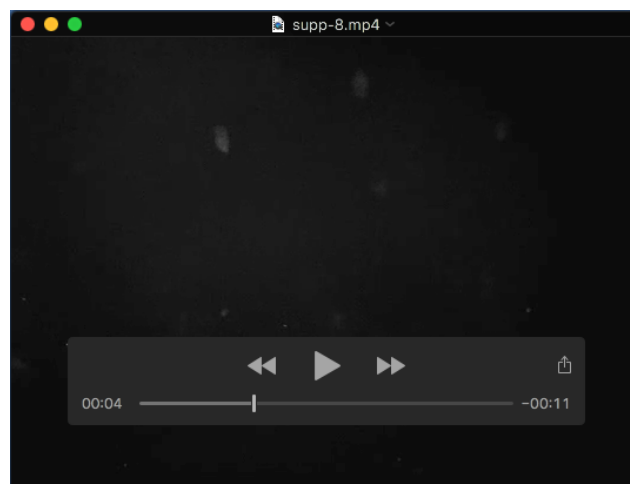
**Figure S6 Details of the different isoform specific *Fas2* mutations**

The figure shows the mutations generated using CRISPR/Cas9. The PAM and the target sequence are indicated by shading. The triangle indicates the predicted cleavage sites. The underlined triplets encode amino acids that can be used for GPI-anchor addition.



### Movie 1

Stage 14 control embryo carrying a *repo-stGFP* element to label glial nuclei.



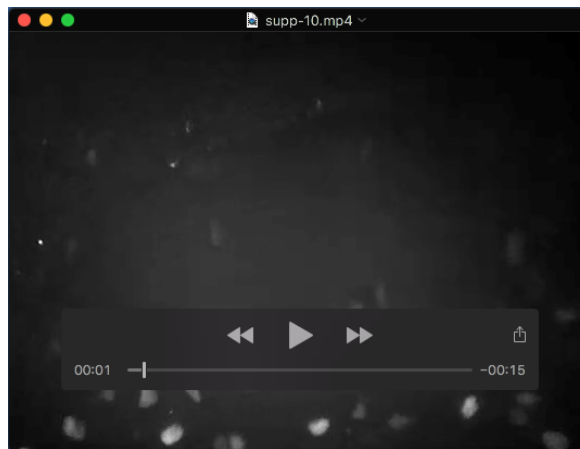
### Movie 2

Stage 14 *Fas2*<sup>EB112</sup> mutant embryo carrying a *repo-stGFP* element to label glial nuclei.



### Movie 3

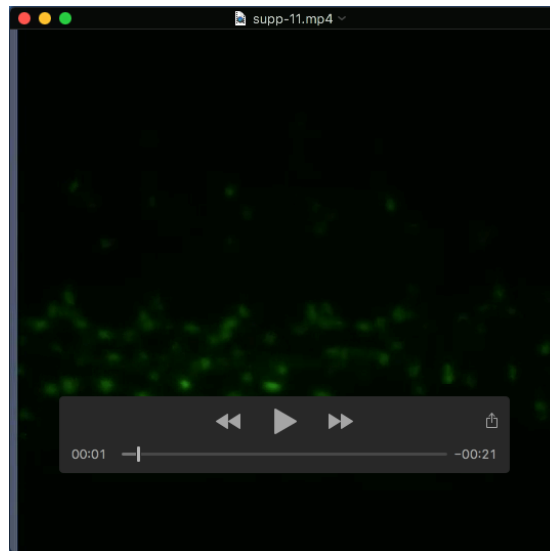
Stage 14 *Df(1)Fas2* mutant embryo carrying a *repo-stGFP* element to label glial nuclei.



### Movie 4

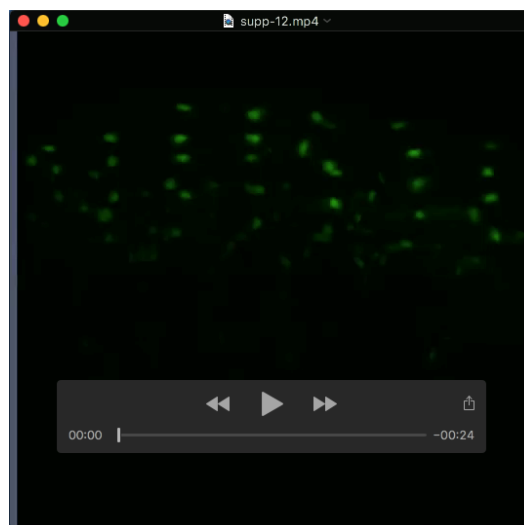
Stage 14 *Fas2<sup>aa</sup>* mutant embryo carrying a *repo-stGFP* element to label glial nuclei.





### Movie 5

Stage 14 *Fas2*<sup>aa</sup> mutant embryo carrying a *repo-stGFP* element to label glial nuclei.



### Movie 6

Stage 14 *Fas2*<sup>aa</sup> mutant embryo carrying a *repo-stGFP* element to label glial nuclei.